Available online at www.sciencedirect.com
SCIENCE DIRECT
Journal of Organometallic Chemistry 691 (2006) 2125–2154
Journal of Organometallic Chemistry
www.elsevier.com/locate/jorganchem

Review

Substituent electronic effects in chiral ligands for asymmetric catalysis

Susan P. Flanagan, Patrick J. Guiry *

Centre for Synthesis and Chemical Biology, UCD School of Chemistry and Chemistry Biology, Conway Institute of Biomolecular and Biomedical Research, University College Dublin, Belfield, Dublin 4, Ireland

Received 20 January 2006; accepted 20 January 2006
Available online 24 March 2006

Abstract

The majority of reports of ligand modification for catalysis have followed from systematic variation of the spatial demands of the catalyst. The focus of this review is to highlight selected major contributions to the area of substituent controlled electronic-tuning of some well known chiral ligands and the subsequent effect of these changes during asymmetric catalysis. The ligand types discussed include the salens, phosphites and phosphoramidites, ferrocene-containing ligands, oxazolines and axially chiral ligands. For each ligand type we attempt analyse the effect of systematic variation of electronics and note whether any improvements in catalyst activity and selectivity are obtained.
© 2006 Elsevier B.V. All rights reserved.

Contents

1. Introduction . . . 2125
2. Salen-type ligands . . . 2126
3. Phosphites and phosphoramidites . . . 2130
4. Ferrocene-containing ligands . . . 2136
5. Oxazoline- and imidazoline-containing ligands . . . 2141
6. Diphosphine and phosphinamine ligands . . . 2145
7. Axially chiral phosphines . . . 2147
8. Conclusion . . . 2153
References . . . 2153

1. Introduction

The design of chiral ligands to impart stereochemical information onto metal-catalysed reactions has become a highly specialised topic of research in organic chemistry. Careful consideration is required when choosing a ligand to promote a particular asymmetric transformation and, even then, success is not guaranteed. More often than not, some degree of fine-tuning of the catalyst scaffold is necessary to ensure a positive outcome. The majority of reports of ligand modification have followed from systematic variation of the spatial demands of the catalyst. Less common are instances of the manipulation of ligand electronic properties, despite the fact that such changes can be, in many cases, implemented with as much ease as steric

* Corresponding author. Fax: +353 17162501.
E-mail address: p.guiry@ucd.ie (P.J. Guiry).

0022-328X/$ - see front matter © 2006 Elsevier B.V. All rights reserved.
doi:10.1016/j.jorganchem.2006.01.063

alterations and produce similarly dramatic improvements in catalyst activity and selectivity. The focus of this review is to highlight major contributions, in the opinion of the authors, to the area of substituent controlled electronic-tuning of some well known ligand classes and the subsequent effect of these changes during asymmetric catalysis, complemented by mechanistic investigations involving kinetic studies, X-ray crystallography and NMR and IR spectroscopy. Examples of ligand electronic effects for heterobidentate ligands where the effect in asymmetric catalysis arises from the differences in the donor atoms themselves fall outside of the scope of this review.

2. Salen-type ligands

Electronic tuning of ligands can be particularly relevant to catalytic transformations such as olefin epoxidation and cyclopropanation that do not involve substrate precoordination and hence are less influenced by the steric bulk of the ligand. Electronic effects in ligands designed for asymmetric epoxidation were initially investigated in 1991 by Jacobsen [1]. Ligands **1a**–**e**, bearing different substituents in the 5,5′-positions, were employed in the asymmetric epoxidation of 2,2-dimethylchromene, *cis*-β-methylstyrene and *cis*-2,2-dimethyl-3-hexene. Linear Hammett plots correlating enantioselectivity with ligand substituent σ_p values were obtained for each substrate. In all cases the enantioselectivity was best for electron-donating ligands, with the observed range of enantiomeric excesses depending on the substrate used. The largest effect was observed for 2,2-dimethylchromene **2**, where the enantiomeric excess was 22% with the nitro-containing ligand **1e** and 96% for the methoxy-substituted variant **1a** (see Scheme 1).

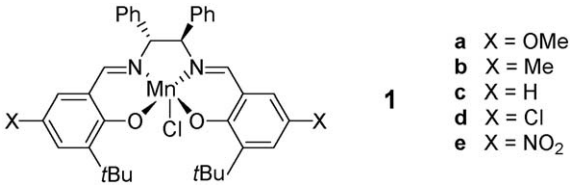

The possibilities of the substituent inciting significant conformational changes in the reactive Mn(V)-oxo intermediates or influencing the Mn-oxo bond lengths and thus affecting the ee of the reaction were deemed unlikely. The explanation proposed by Jacobsen was that substituent effects were manifested as different reactivities of the Mn-oxo intermediates. The electron-withdrawing ligands increase the reactivity of the intermediate and oxygen transfer proceeds with a more reactant-like transition state with relatively low levels of interaction between substrate and catalyst and therefore less steric differentiation between the diastereomeric transition states. Less reactive oxidants, such as those containing electron-rich ligands, deliver the oxygen in a more product-like transition state where the non-bonding interactions are stronger and so a higher enantioselectivity is achieved.

Evidence supporting this hypothesis was reported in a further publication by Jacobsen [2]. Examination of secondary isotope effects involving epoxidation of styrene and *cis*-β-deuteriostyrene with catalysts **1a**–**e** was undertaken to determine the relative position of the transition state along the reaction coordinate. A correlation was obtained between the value of k_H/k_D at C_β (and thus the degree of rehybridisation from sp^2 to sp^3 that accompanies the initial C–O bond formation) with σ_p and the observed enantioselectivity (Fig. 1 and Table 1).

Cis/*trans* product ratios were also evaluated for the epoxidation of *cis*-β-deuteriostyrene and were found to be dependent on the electronic nature of the 5,5′-substituent. This implied that formation of both C–O bonds of the epoxide and hence the selectivity of the reaction were reliant on ligand electronics. Linear Hammett plots were also obtained in a study of epoxidation of indene over a 100 °C temperature range. Significantly, an "isoelectronic" point was detected which indicates that a single reaction parameter

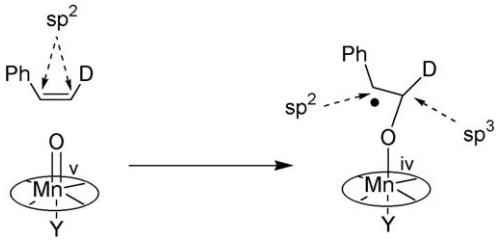

Fig. 1. Mechanism of epoxidation of *cis*-β-deuteriostyrene.

Table 1
Isotope effects in the epoxidation of styrene and *cis*-β-deuteriostyrene

Entry	Catalyst	k_H/k_D	Enantiofacial selectivity[a]	*Cis*/*trans*[a]
1	**1a** (X = OMe)	0.82	5.4	5.1
2	**1b** (X = Me)	0.84	4.8	5.7
3	**1c** (X = H)	0.86	4.4	6.3
4	**1d** (X = Cl)	0.90	4.2	6.9
5	**1e** (X = NO_2)	0.95	2.0	7.1

[a] Determined by ^1H NMR in the presence of chiral shift reagent ($Eu(hfc)_3$) according to: enantiofacial selectivity = [*cis* + *trans* (major enantiomers)]/[*cis* + *trans* (minor enantiomers)].

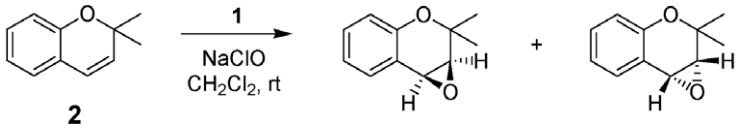

Scheme 1.

(such as degree of bond formation and thus transition state position) is influenced by the 5,5′-substituent.

Gilheany and co-workers have carried out extensive investigations into the asymmetric epoxidation of *trans*-β-methylstyrene using oxo-chromium(V)-salen complexes **2**, Scheme 2 [3,4].

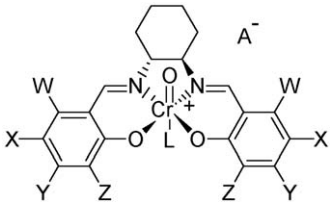

2

(For A⁻, W, X, Y, Z see Table 2)

Since substitution at the 3,3′-positions (Z) on the salen rings was known to be important to induce high enantioselectivity, they initially focused on varying the substituent at this position, Table 2. The results showed that in the presence of a suitable donor ligand L, any substituent at the 3,3′-position, regardless of size, is sufficient to provide enantiomeric excesses ⩾80%. Reaction rates were greatest for complexes bearing electron-withdrawing substituents, owing to the fact that the reaction mechanism involves electrophilic attack of chromium on the alkene. The fast reaction time of the methoxy-substituted Cr-species was due to decomposition of the complex rather than high reactivity. Higher yields were obtained with the electron-withdrawing halogen-substituted catalysts than for the alkyl-substituted analogues, which were attributed to the faster reaction rates allowing for less decomposition of catalyst.

Introducing a chloro-substituent in the Y- or X-positions led to no change or a reduction in selectivity, Scheme 3 and Table 3, entries 1 versus 3 and 4, 2 versus 6 and 7, 4 versus 9, 3 versus 9, 8 versus 11, whereas substitution at W, in the absence of a Z-substituent resulted in an increased ee, entries 1 versus 5, 4 versus 10. However, there was no cooperative effect noted between W- and Z-substitution, leading to the conclusion that substituents at the Z-position have a greater influence on the conformation of the chromium complex. The non-cooperativity was also suggested to imply that altering the substituent at the two different positions (W and Z) might independently affect two different pathways of approach of the substrate.

Improved enantioselectivities were observed using oxo-chromium complexes derived from the trifluoromethyl-substituted salen ligand, **3** [5]. With triphenylphosphine oxide as donor ligand, the enantioselectivity reached 92%, which was the highest ee reported for a metal-mediated epoxidation of a *trans*-alkene.

Mezzetti and co-workers have initiated an examination of the effect of electronic tuning of a PNNP ligand used

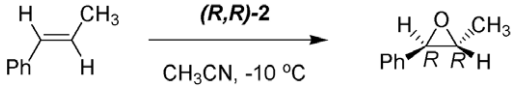

Scheme 2.

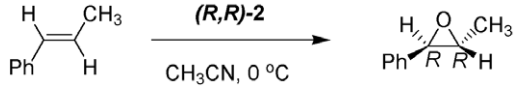

Scheme 3.

Table 2
Epoxidation of *trans*-β-methylstyrene

L[a]	Ee[b] (%) and Yield[b] (%) (in italics) for various Z[c]						
	H	OMe[d]	Me	*t*-Bu	Ph	Cl	F
None	58	49 *6*	78 *8*	84 *16*	66 *12*	80 *27*	70 *39*
Ph_3PO	72	58 *17*	82 *12*	79 *17*	85 *14*	86 *43*	86 *45*
4PhPyNO[e]	67	52 *9*	70 *10*	70 *19*	69 *12*	74 *23*	85 *16*
DMF	69	57 *9*	77 *14*	78 *13*	77 *15*	78 *48*	nr
Time[f]	12 h	10 m	2 d	7–10 d	2 d	30 m	1 h

[a] (*R*,*R*)-**2** (40–60 mg, 1 equiv.), CH_3CN (3 mL), donor L (1 equiv.), iodosylbenzene (1.2 equiv.), cooled to −10 °C, *trans*-β-methylstyrene, (1 equiv).
[b] Determined by chiral GC.
[c] W, X, Y = H.
[d] Room temperature, donor L and alkene added before iodosylbenzene.
[e] 4-phenylpyridyl-*N*-oxide.
[f] Time of discharge of green colour to orange.

Table 3
Epoxidation of *trans*-β-methylstyrene

Entry[a]	Salen Substituent[b]				Time[c]	Ee[d] for L	
	W	X	Y	Z		None	Ph_3PO
1[e]	H	H	H	H	12 h	58	72
2				Cl	1 h	80	85/88[f]
3			Cl		1 h	61[f]	66/68[f]
4[e]		Cl			50 min	58	71
5	Cl				2 h	72/69[f]	74/80[f]
6[g]			Cl	Cl	1 h	69	70
7[e]		Cl		Cl	1 h	67	83
8	Cl			Cl	15 min	75	82
9		Cl	Cl		1 h	59	61
10	Cl	Cl			1 h	68	69
11	Cl	Cl		Cl	10 min	68	72
12[e]	Cl	Cl	Cl	Cl	5 min	48	62

[a] (*R*,*R*)-**2** (40–60 mg, 1 equiv.), CH_3CN (3 mL), iodosylbenzene (1.2 equiv.), donor L (1 equiv.), cooled to 0 °C, *trans*-β-methylstyrene (1 equiv.).
[b] Unspecified substituents are H.
[c] Time to discharge of green colour to orange.
[d] Determined by chiral GC.
[e] At −10 °C.
[f] A = NO_3^-, PF_6^- otherwise.
[g] In dichloromethane.

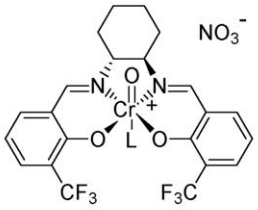

3

L = Ph_3PO, pyridine *N*-oxide, DMF, DMSO

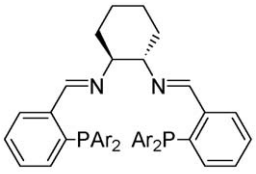

4 **a** Ar = C_6H_5 **b** Ar = 4-$CF_3C_6H_4$

for the Ru-mediated asymmetric cyclopropanation of olefins [6]. The ligands synthesised for their study were **4a** and its 4-trifluoromethyl derivative **4b**. In previous work by the researchers complexes of the type [RuCl(PNNP)]PF_6 had provided their most active and selective catalysts [7]. However, due to the electron-deficient nature of the ligand **4b** reducing the electron density at the metal centre, the removal of Cl from **5** to yield penta-coordinated **6** was unsuccessful. Abstraction of the chloride from **5** was possible with stabilisation of the resultant species with oxygen-donor ligands such as ether, triflate and water to form complexes **7**–**9**, Fig. 2. The formation of adducts with oxygen donors was known to reduce selectivity, which would possibly partially suppress the beneficial effects of making the ligand more electron-deficient.

The Ru-complexes were then screened in the cyclopropanation of styrene, α-methylstyrene and 1-octene, Scheme 4. For styrene as substrate, in some cases catalyst activity improved with the inclusion of the 4-trifluoromethyl-substituent, Table 4, entries 3 versus 2, although in general, use of water as adduct lowered the yield significantly. Changing the counterion to BArF [B(4-$CF_3C_6H_4)_4$] did improve the conversion and diastereoselectivity for the more electron-deficient ligand with a loss in ee of 9%, whereas it had a detrimental effect on the performance of the unsubstituted variant, decreasing the ee from 91% to 34%, entry 4 versus 6. The triflato complexes of the 4-trifluoromethyl-substituted PNNP ligand were completely inactive in cyclopropanation, whereas a yield of 20%, accompanied by modest selectivity, was achievable using the unmodified ligand, compare entries 8 to 9.

When the ether adduct **8b** was tested in the cyclopropanation of α-methylstyrene **10**, it provided an enhanced *cis*:*trans* ratio and much improved enantioselectivity in comparison to its unsubstituted counterpart, Scheme 5

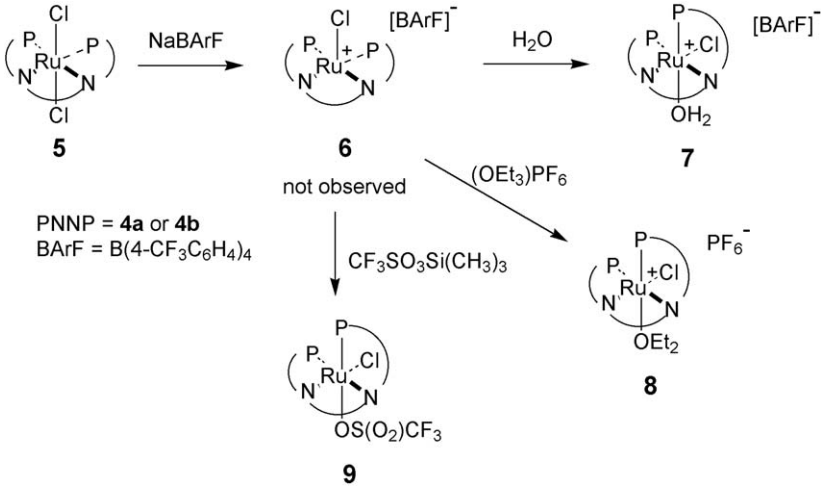

Fig. 2. Ru complexes of PNNP ligands.

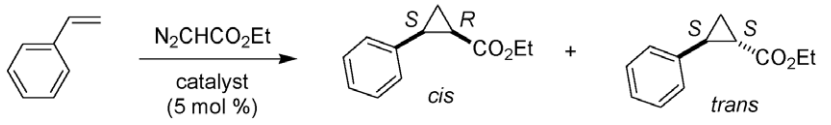

Scheme 4.

Table 4
Cyclopropanation of styrene

Entry[a]	Complex	Conv. (%)	Yield (%)	*cis*:*trans*	Ee (%)	
					cis	*trans*
1[c]	[Ru(Cl)**4a**]PF_6	70	41	91:9	87	24
2	[RuCl(OEt_2)**4a**]PF_6	73	28	84:16	80	0
3	[RuCl(OEt_2)**4b**]PF_6	80	54	90:10	83	4
4	[RuCl(OH_2)**4a**]PF_6	61	28	86:14	91	8
5	[RuCl(OH_2)**4b**]PF_6	34	17	93:7	89	15
6[b,c]	[RuCl(OH_2)**4a**]BArF	56	12	72:28	34	39
7[b]	[RuCl(OH_2)**4b**]BArF	84	35	98:2	80	13
8	[RuCl(η^1-O_3SCF_3)**4a**]	53	20	75:25	64	3
9	[RuCl(η^1-O_3SCF_3)**4b**]	0	0	–	–	–
10	[RuCl(OH_2)**4b**](O_3SCF_3)	68	9	92:8	90	1

[a] Reaction conditions: ethyl diazoacetate (0.96 mmol, 2 equiv vs. olefin, unless otherwise stated) in CH_2Cl_2 (1 mL) added over 6 h to a CH_2Cl_2 solution of styrene (0.48 mmol) and catalyst (24 μmol, 5 mol%). Reaction time 20 h.
[b] 1 equiv. ethyl diazoacetate (0.48 mmol) used.
[c] Catalyst is 1:1 mixture of [**7a**]BArF and **6a**.

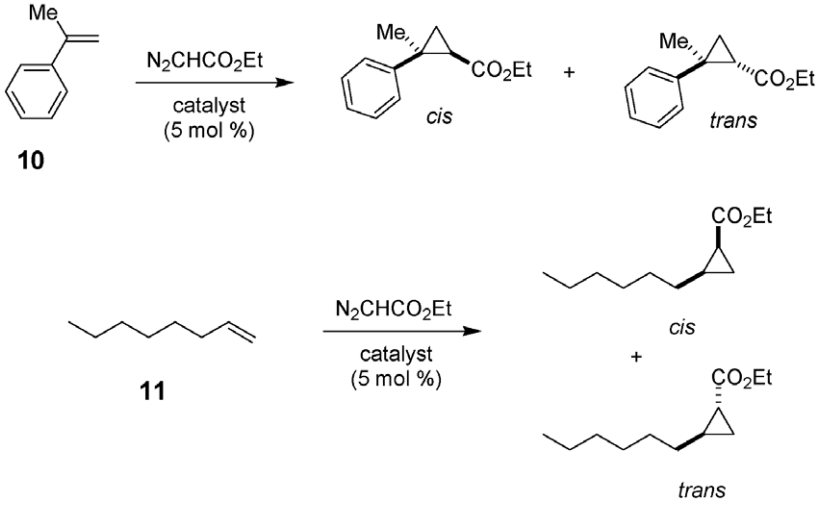

Scheme 5.

Table 5
Cyclopropanation of α-methylstyrene and 1-octene

Entry[a]	Substrate	Complex	Yield[b] (%)	*cis*:*trans*	Ee[c] (%)	
					cis	*trans*
1	**10**	[RuCl(OEt_2)**4a**]PF_6	90	76:24	23	18
2	**10**	[RuCl(OEt_2)**4b**]PF_6	94	85:15	86	34
3	**11**	[RuCl(OH_2)**4a**]PF_6	30	60:40	47 (1*R*,2*S*)	20 (1*S*,2*S*)
4	**11**	[RuCl(OEt_2)**4b**]PF_6	54	76:24	43 (1*R*,2*S*)	13 (1*S*,2*S*)

[a] Reaction conditions: ethyl diazoacetate (1.92 mmol, 2 equiv. vs. olefin) in CH_2Cl_2 (2 mL) added over 6 h to a CH_2Cl_2 solution of substrate (0.96 mmol) and catalyst (48 μmol, 5 mol%). Reaction time 20 h.
[b] Yields refer to isolated product as the sum of *cis* and *trans* isomers.
[c] Absolute configuration not determined.

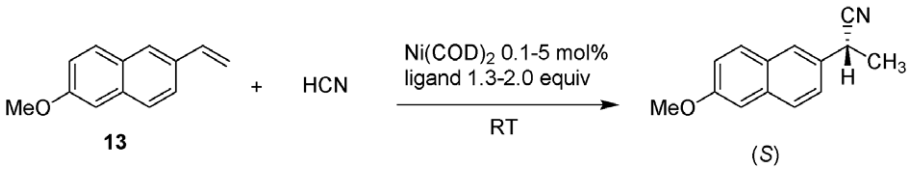

Scheme 6.

and Table 5, entry 2 versus 1. A higher yield and better diastereoselectivity were obtained for 1-octene **11** as substrate, albeit with a lower ee, entry 4 versus 3. However, at the time of the report there were no catalytic systems displaying *cis*-selectivity in the cyclopropanation of alkyl substituted olefins and so it was maintained that further electronic tuning of the PNNP ligands could yield desirable results.

3. Phosphites and phosphoramidites

RajanBabu reported the application of sugar-derived phosphinite ligands in the Ni(0)- catalysed asymmetric Markovnikov addition of HCN to vinylarenes [8,9]. In particular, derivatives of β-phenyl glucoside were synthesised, wherein the steric and electronic properties at a number of sites on the ligand were varied to optimise the enantioselectivity of the reaction.

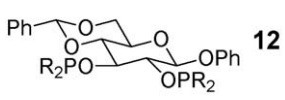

12

a R = C_6H_5
b R =3,5-$Me_2C_6H_3$
c R =3,5-$F_2C_6H_3$
d R =3,5-$(CF_3)_2C_6H_3$

The substrate examined in this initial study was 6-methoxy-2-vinylnaphthalene (MVN) **13**, a precursor to the anti-inflammatory drug Naproxen, Scheme 6. The transformation proceeded with up to 100% conversion, with total regioselectivity in favour of the branched product and, while substituent tuning at the glycoside bond led to some improvement of the ee, a more pronounced effect was noted by changing the substituents on the phosphorus aryl groups, Table 6. It was found that placing trifluoromethyl substituents on the aryl groups dramatically increased the enantioselectivity and also the catalytic activity of the Ni-based system, compare entries 2 and 4.

The electronic effect was not confined to ligands containing *meta*-substituted aryl groups. *para*-Methoxy, *para*-fluoro and *para*-trifluoromethyl substituted ligands gave ees of 17%, 38% and 65%, respectively, in the Ni-catalysed hydrocyanation of **13** in hexane, following the trend of improved enantioselectivity with increasing electron-withdrawing capacity [10]. Other substrates also highlighted the importance of the electronic nature of the ligand. Striking differences in the enantioselectivity obtained by the ligands containing unsubstituted and trifluoromethyl-

Table 6
Hydrocyanation of 6-methoxy-2-vinylnaphthalene (**13**)

Entry	Ligand	Solvent	Ee (%)
1	**12a**	Benzene (THF)	40 (29)
2	**12b**	Benzene	16
3	**12c**	Hexane	77
4	**12d**	Benzene	78
5	**12d**	Hexane or C_6F_6	85
6[a]	**12d**	Hexane	91

[a] Reaction performed at 0 °C.

Table 7
Hydrocyanation of vinylarenes

Entry	Substrate	Ee (%)		
		12a	**12c**[c]	**12d**
1[a]	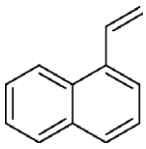	63	–	68
2[a]	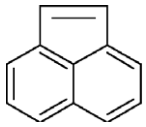	0	–	59
3[a]	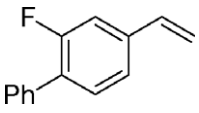	10[d]	–	55
4[b]	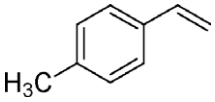	1	47	70
5[b]	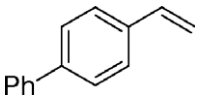	8	41	68
6[b]	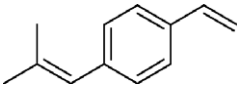	–	–	63
7[b]	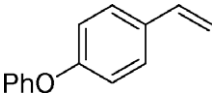	7	38	60
8[b]	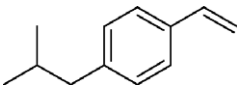	6	38	56
9[b]	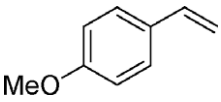	6	39	52
10[b]	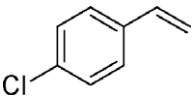	–	–	40
11[b]	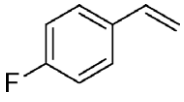	4	15	28
12[b]	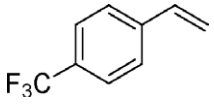	1	9	14

[a] 0.10–0.20 M alkene, 1.0–5.0 mol% $Ni(COD)_2$/ligand in hexane.
[b] 0.65 mmol alkene, 0.020 mmol $Ni(COD)_2$ 0.020 mmol ligand, hexane.
[c] Not recorded.
[d] Reaction performed in benzene.

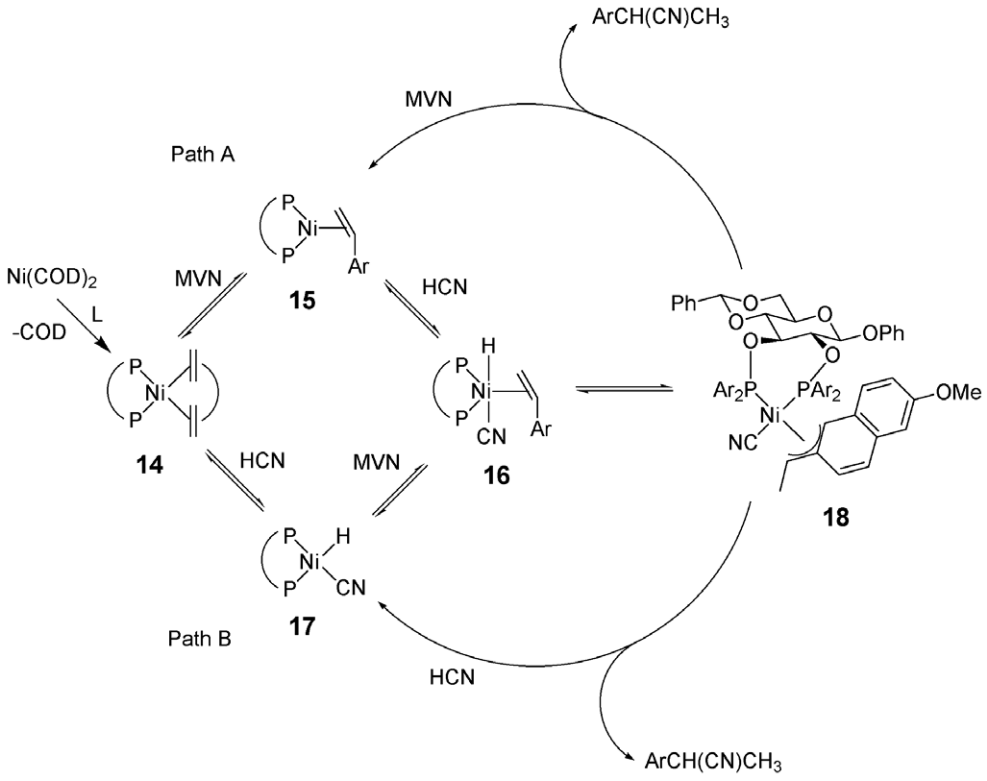

Scheme 7.

substituted aryl groups were observed, especially for the hydrocyanation of acenapthalene and *para*-methylstyrene, Table 7, entries 2 and 4.

In order to obtain a deeper understanding of the origin of the increase in enantioselectivity through the use of more electron-deficient ligands, kinetic studies, ^{31}P NMR analysis of key reaction intermediates, examination of the individual carbonyl stretching frequencies in IR spectra of $Ni(CO)_2$ligand complexes and deuterium labelling techniques. The overriding implications of that study, which proposed a catalytic cycle, Scheme 7, were that (a) the relative rates of formation of the diastereomeric complexes of **15** (**15$_R$** and **15$_S$**, Scheme 8) were most likely equilibrated during hydrocyanation, and therefore their ratios did not directly influence the enantioselective outcome and (b) the primary effect of the electron-withdrawing aryl-substituents was to decrease the electron-density at nickel thereby increasing the rate of reductive elimination of the product nitrile from the (η^3-benzyl)nickel cyanide complex **18**, with the diastereomer leading to the observed major enantiomer of product being affected to the greater extent.

The glucose-derived diarylphosphinites were also utilised in the rhodium-catalysed hydrogenation of dehydroamino acids to form the corresponding L-amino acids, Scheme 9 [11]. Once again, a substantial dependence on the electronic nature of the ligand was observed although, unlike the Ni-catalysed hydrocyanations, more electron-rich phosphinites gave the highest enantioselection, Table 8, column **12b** versus **12c** and **12d**.

Access to D-amino acids was obtained after structural variations of the backbone of the D-glucose ligand systems used to generate the L-amino acids. Thus, ligands **19** were prepared and their electronic effects on the Rh-catalysed hydrogenation of phenylalanine were studied, Scheme 10. As expected from the results obtained using ligands **12**, the more electron-rich variants, namely **19b** and **19f** gave far greater enantioselectivities than the electron-poor ligands **19c** and **19d**.

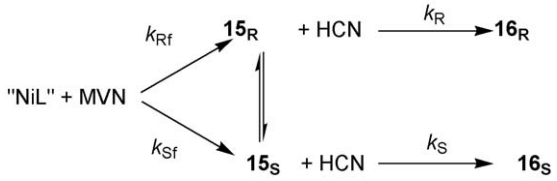

Scheme 8.

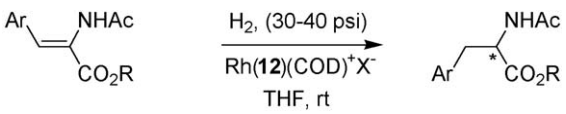

Scheme 9.

Table 8
Rh-catalysed hydrogenation of dehydroamino acids

Entry	Substrate	Ee[a] (%)			
		12a	**12b**	**12c**	**12d**
1	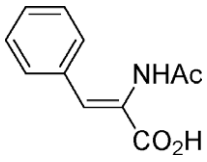	94.0	99.0	60.0	71.0
2	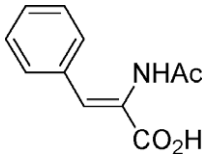	91.0	97.0	53.0	5.0
3	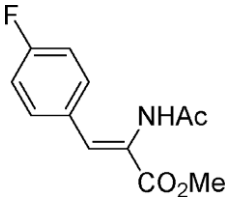	85.0	97.2	13.0	9.0
4	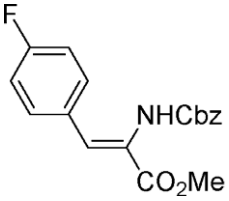	62[b]	97[b]	<1[b]	54[b]

[a] Ee determined by GC analysis on methyl esters.
[b] Ee determined by HPLC after reduction on alcohols.

In a more recent examination of the electronic effects of the phosphinite ligands on Rh-catalysed hydrogenation, RajanBabu et al. synthesised C_2-symmetric diarylphosphinites **20** based on enantiomerically pure *trans*-1,2-cyclohexanediol [12]. The same aryl groups used in the variation of **19** were incorporated into ligands **20**. Using C_2-symmetric ligands minimises the number of possible diastereomeric intermediates formed during the catalytic cycle thus reducing the influence of their relative concentrations and reaction rates on the enantioselectivity generated. This allows for a better assessment of the electronic influence of the ligand on the reaction.

20

During the hydrogenation of N-acetyl-phenylalanine-methyl ester, the trend of achieving higher enantioselectivity with catalysts derived from more electron-rich phosphinites was noted (82% ee with Ar=Ar′=3,5-$Me_2C_6H_3$ versus 26% ee with Ar=Ar′=3,5-$(CF_3)_2C_6H_3$). To gain insight into the manner in which the electronics of the system was affecting the results, crystal structures of the precatalysts with electronically different diarylphosphinites were determined. Ground state conformations of Rh complexes containing both electron-rich and electron-poor ligands were structurally similar despite the fact that widely different enantioselectivities arose from their application in catalysis. This implied that the electronic enhancement of ee was not due to changes in ground state conformations.

Variable-temperature ^{31}P NMR studies of (dimethylitaconate)Rh^+(phosphinite ligand) synthesised with both electron-rich and electron-deficient ligands were undertaken to attempt to determine the relative concentrations of the two diastereomeric species present in solution. A higher ratio of major to minor diastereomer was indeed observed for the more electron-rich (more selective) 3,5-dimethylphenylphosphinite than for the unsubstituted

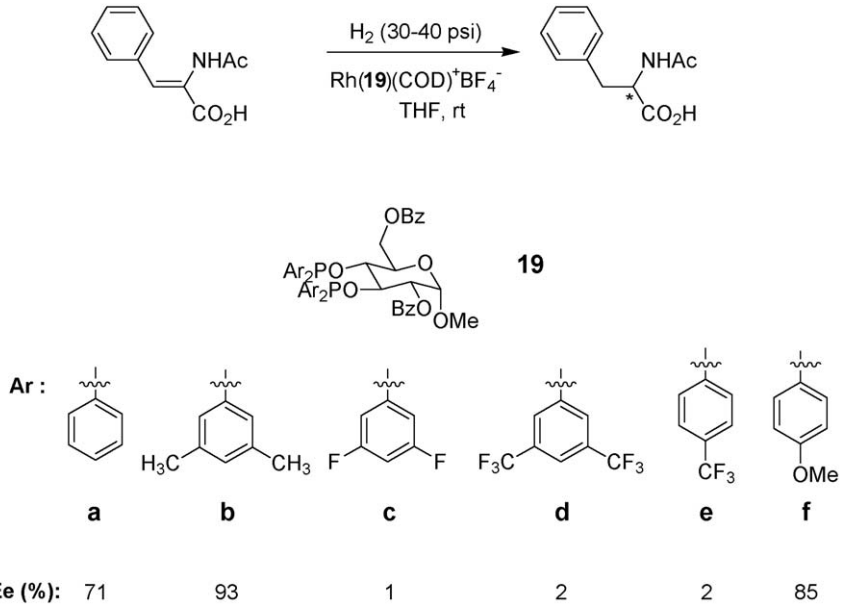

Scheme 10.

diphenylphosphinite but in the case of the more electron-poor 3,5-difluoro and 3,5-di(trifluoromethyl) systems, the diastereomeric ratios could not be clearly established.

The range of phosphinite ligands applied to the Ni-catalysed hydrocyanation of **13** was extended to include fructofuranoside derivatives **21**, which afford the (*R*)-enantiomer of product in excess [13]. The steric effects were largely kept constant and the electronic effects were varied. Again, it was found that electron-donating substituents on the phosphorus aryl groups induced the lowest enantiomeric excesses, Table 9, entries 5 and 8. Changing to more electron-poor ligands produced a small improvement, entries 2 and 10, but the electronically asymmetric ligand systems proved the most successful, with the ee reaching 95% at 0 °C, entry 4. In this case the more electron-deficient phosphinite was at C_4 and the more electron-rich one at C_3, which appeared to be the general requirement for high enantioselectivity using these ligands.

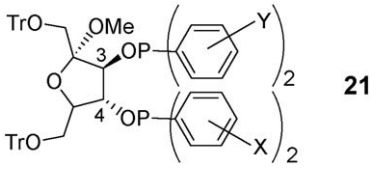

21

Table 9
Ni-catalysed hydrocyanation of 6-methoxy-2-vinylnapthalene (**13**)

Entry	Ligand	X	Y	Ee (%) (*R*)
1	**21a**	H	H	43
2	**21b**	3,5-$(CF_3)_2$	3,5-$(CF_3)_2$	56
3	**21c**	H	3,5-$(CF_3)_2$	58
4	**21d**	3,5-$(CF_3)_2$	H	89 (95 at 0 °C)
5	**21e**	4-OMe	4-OMe	25
6	**21f**	3,5-$(CF_3)_2$	4-OMe	84
7	**21g**	3,5-$(CF_3)_2$	4-F	88
8	**21h**	3,5-Me_2	3,5-Me_2	40
9	**21i**	3,5-$(CF_3)_2$	3,5-Me_2	78
10	**21j**	3,5-F_2	3,5-F_2	45
11	**21k**	H	3,5-F_2	40
12	**21l**	3,5-F_2	H	63
13	**21m**	3,5-F_2	3,5-Me_2	42
14	**21n**	3,5-$(CF_3)_2$	3,5-F_2	78

The same principle of electronic asymmetry was applied to the simpler phosphinites **22** synthesised from the C_2-symmetric diol, (*S*,*S*)-tartranil, **23**. The enantioselectivies achieved in the Ni-catalysed hydrocyanation of the Naproxen precursor **13** were reasonable but the improvement on going from symmetric to asymmetric ligands was not as pronounced as for ligands **21**, Scheme 11.

Bakos and co-workers have applied new and previously prepared BINOL- and H_8-BINOL-related phosphites **24** and **25** to Rh-catalysed asymmetric hydrogenation of alkenes [14,15].

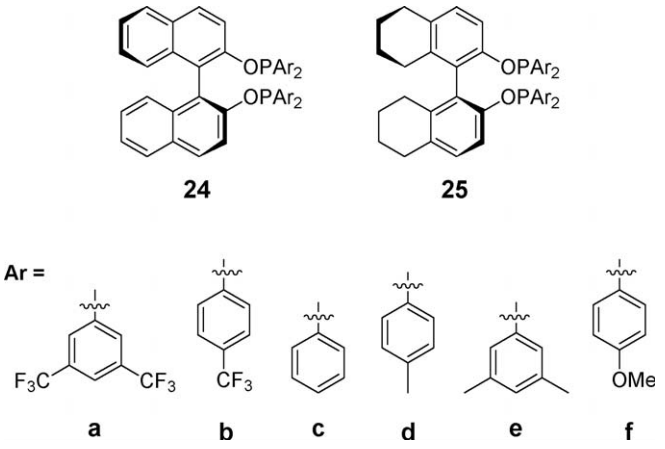

As RajanBabu had found with his ligand systems, the introduction of electron-rich aryl groups onto the phosphorus donor atom enhances both the enantioselectivity and catalyst activity during hydrogenation of dimethyl itaconate relative to the sterically similar electron-poor analogues, Scheme 12, Table 10, entries 4 and 5 versus 1 and 2.

Methyl (*Z*)-α-acetamidocinnamate was also subjected to Rh-catalysed hydrogenation using ligands **24** and **25**, Scheme 13. Poorer catalyst activity was noted for the electron-poor ligands accompanied by low enantiomeric excesses, Table 11, entries 1 and 2. The electron-rich catalysts proved highly efficient in promoting the transformation with reactions reaching completion after less than 30 min in most cases and enantiomeric excesses of up to 98.6% being obtained, entries 3–6.

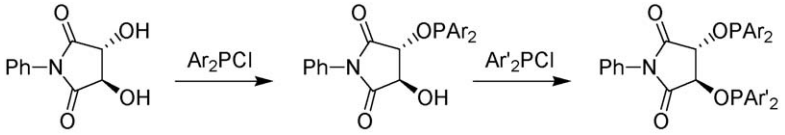

(*S*,*S*)-**23**

(*S*,*S*)-**22** **ee %** (*S*)

a Ar = Ar' = Ph 54
b Ar = Ar' = 3,5-$(CF_3)_2C_6H_3$ 70
c Ar = Ph; Ar' = 3,5-$(CF_3)_2C_6H_3$ 77

Scheme 11.

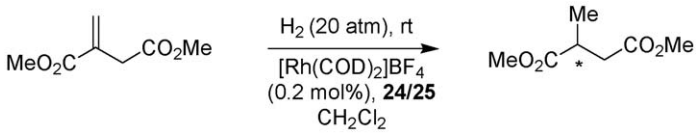

Scheme 12.

Table 10
Rh-catalysed hydrogenation of dimethyl itaconate

Entry	Ligand	Ar	Time (min)	Conv. (%)	Ee (%) (*R*)
1	**24a** (**25a**)	3,5-$(CF_3)_2C_6H_3$	90 (90)	87.7 (82.3)	51.6 (50.9)
2	**24b** (**25b**)	4-$CF_3C_6H_4$	20 (30)	100 (100)	72.9 (65.6)
3	(**25c**)	C_6H_5	(17)	(100)	(81.3)
4	**24d** (**25d**)	4-MeC_6H_4	7 (10)	100 (100)	89.5 (81.0)
5	**24e**	3,5-$Me_2C_6H_3$	9	100	91.5
6	**24f**	4-$MeOC_6H_4$	5	100	92.2
7	**24f**	4-$MeOC_6H_4$	25	100	93.9[a]

[a] H_2 pressure of 1 atm.

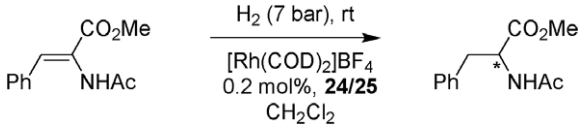

Scheme 13.

Table 11
Rh-catalysed hydrogenation of methyl (*Z*)-α-acetamidocinnamate

Entry	Ligand	Ar	Time (min)	Conv. (%)	Ee (%) (*S*)
1	**24a**	3,5-$(CF_3)_2C_6H_3$	105	29.3	30.9
2	**24b**	4-$CF_3C_6H_4$	50	81.8	48.7
3	**24d**	4-MeC_6H_4	25	100	92.5
4	**24e** (**25e**)	3,5-$Me_2C_6H_3$	13 (25)	100 (100)	95.4 (93.9)
5	**24f**	4-$MeOC_6H_4$	6	100	96.8
6	**24f**	4-$MeOC_6H_4$	25	97.5	98.6[a]

[a] H_2 pressure of 1 atm.

Ligands **24** and **25a**, **b**, **d** and **e** were also screened in the rhodium-catalysed hydroformylation of styrene, Scheme 14 and Table 12 [16].

Although the enantiomeric excesses achieved were extremely poor in some most cases, an enhancement was obtained in replacing the 3,5-dimethyl substituted phosphonites with the more basic 3,5-bis(trifluoromethyl)-substituted ligands, compare entries 1,4 and 5,8. Conversions and turnover frequencies are also affected by the electronic nature of the aryl group, with the rate of reaction increasing with increasing substituent electron-withdrawing power.

Table 12
Rh-catalysed hydroformylation of styrene

Entry	Ligand	Conv. (%)	TOF[a]	*b*/*l* Ratio[b]	Ee (%)[c]
1	**24e**	10	212	82/18	2 (*S*)
2	**24d**	6	114	86/14	1 (*S*)
3	**24b**	18	358	79/21	3 (*S*)
4	**24a**	62	1236	41/59	50 (*S*)
5	**25e**	7	134	78/22	9 (*S*)
6	**25d**	19	380	86/14	1 (*S*)
7	**25b**	28	566	73/27	3 (*S*)
8	**25a**	66	1310	37/63	30 (*S*)

[a] Amount of RCHO in mol (mol Rh)$^{-1}$ h^{-1} determined at 1 h.
[b] Branched/linear product ratio.
[c] Determined by GC of the distilled product.

[Rh(ligand)(CO)Cl] complexes were prepared for each of the eight ligands tested and their corresponding carbonyl IR stretching frequencies were compared. As expected, those compounds containing electron-withdrawing ligands (and therefore electron-deficient rhodium atoms which are less capable of back-bonding to the carbonyl group) showed higher CO stretching frequencies in the same order observed for the ligand reactivities.

In contrast to the improvement of ee by switching to more electron-poor ligands, the regioselectivity of the

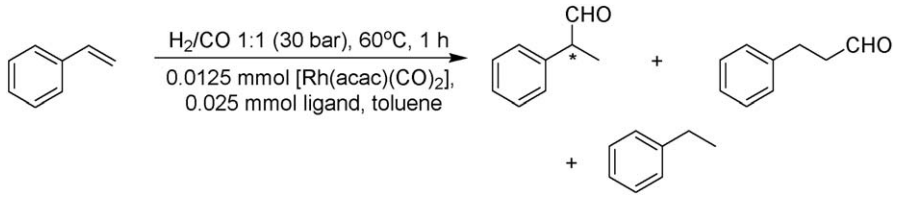

Scheme 14.

reaction was adversely affected, entry 4 versus 1. Bakos postulated that this was due to the fact that the more electrophilic rhodium centre generated after coordination of ligands **24a** and **25a** is more reactive towards CO dissociation and β-hydride elimination leading to increased levels of linear product.

Zhou and co-workers have recently developed the monodentate phosphoramidite SIPHOS **26a** and the structurally-related phosphonite ligands **26b–d** from optically pure (*S*)-SPINOL [17,18].

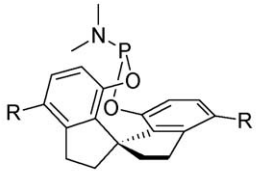

26

a R = H (**SIPHOS**)
b R = Br
c R = Ph
d R = OMe

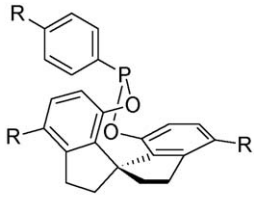

27

a R = H; **b** R = Me;
c R = OMe; **d** R = Cl;
e R = CF_3

The use of the phosphoramidite ligands **26a–d** in the Rh-catalysed hydrogenation of enamides **28** and 2-acetamidocinnamic esters **29** proceeded with excellent enantioselectivity (>95%) and full conversion for almost all combinations of ligand and substrate. The lowest ee's (by 2–4%) were obtained using the 4,4′-dimethoxy SIPHOS **26d**, indicating that electron-donating substituents at this position slightly reduce the asymmetry of the reaction.

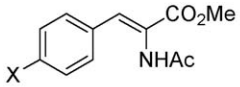

28

X = H, Cl, OMe, NO_2

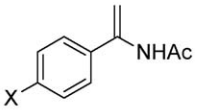

29

X = H, Cl, Me

The weak electronic effect witnessed with the phosphoramidites **26a–d** was attributed to the distal location of the substituents from the metal coordination sphere and prompted the development of the phosphonites **27a–e**, which have an electronically tunable aryl group directly attached to the chelating phosphorus atom. In order to minimise steric interactions the various substituents were introduced in the *para*-position of the phenyl ring. The ligands were then applied in rhodium-catalysed hydrogenation of **30a**, Scheme 15 and Table 13.

From these results, it appears that electron-donating substituents on the aryl group do not have much of an affect on catalytic performance compared to the parent SIPHOS ligand, entries 1–3. Electron-deficient phosphonites **27d** and **27e**, however, produce a lower enantioselectivity and also less active catalysts, requiring up to eight times longer to provide 100% conversion, entry 4 and 5 versus 1. A more pronounced difference was noted for the hydrogenation of (*Z*/*E*)-β-phenyl-β-(acetamino)acrylate **30b**, Table 14, entries 4 and 5 versus 1 (see Scheme 16).

The fact that the lower conversions and enantiomeric excesses obtained using electron-deficient phosphonites could have arisen from poor coordination with rhodium was not overlooked. ^{31}P NMR showed that the coordinations of

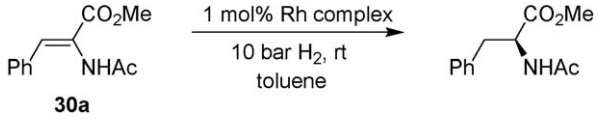

30a

Scheme 15.

Table 13
Rh-catalysed hydrogenation of methyl (*Z*)-α-acetamidocinnamate

Entry[a]	Ligand	R	Time[b] (h)	Ee[c] (%) (*S*)
1	(*S*)-**27a**	H	3	98
2	(*S*)-**27b**	Me	3	97
3	(*S*)-**27c**	OMe	2	99
4	(*S*)-**27d**	Cl	10	93
5	(*S*)-**27e**	CF_3	24	82

[a] $Rh(COD)_2BF_4$/ligand/substrate = 1:2:100.
[b] Time for 100% conversion, quantitative yields in all cases.
[c] Determined by chiral GC.

Table 14
Rh-catalysed hydrogenation of (*Z*/*E*)-β-phenyl-β-(acetamino)acrylate

Entry[a]	Ligand	R	Time (h)	Conv.[b] (%)	Ee[c] (%) (*R*)
1	(*S*)-**27a**	H	40	100	92
2	(*S*)-**27b**	Me	40	100	92
3	(*S*)-**27c**	OMe	40	100	93
4	(*S*)-**27d**	Cl	48	70	87
5	(*S*)-**27e**	CF_3	48	30	40

[a] $Rh(COD)_2BF_4$/ligand/substrate = 1:2:100.
[b] Determined by GC.
[c] Determined by chiral GC.

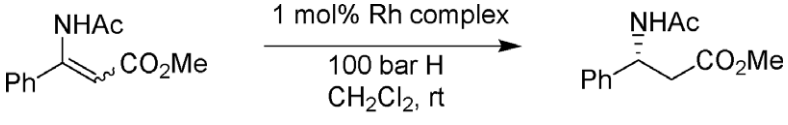

30b

Scheme 16.

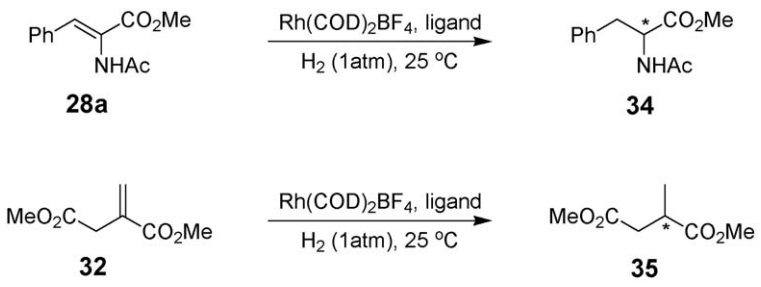

Scheme 17.

the unsubstituted, OMe and CF_3 ligands to rhodium were all complete after 5 min under the normal reaction conditions, thus indicating that the slower reaction rates and lower enantioselectivities of the electron-deficient ligands were mostly due to their electronic characters.

Rh-catalysed hydrogenation of dehydroaminoacids by phosphite ligands has also been investigated by Korostylev and Börner with their acylphosphite ligands **31a**–**b**, Fig. 12 of [19].

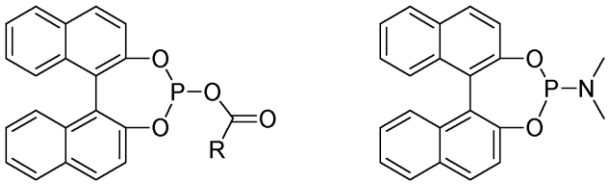

31 **a** R = Me **b** R = Ph

33

They reported moderate enantioselectivities in the Rh-catalysed hydrogenation of methyl 2-acetamido cinnamate **28a** and dimethyl itaconate **32**, Scheme 17, in comparison to the phosphoramidite ligand **33** designed by Feringa et al. [20] and attributed this to the stronger electron-withdrawing nature of the phosphorus acyl substituent relative to the amine substituent, Table 15.

Table 15
Rh-catalysed hydrogenation of methyl-2-acetamidoacrylate

Entry[a]	Substrate	Ligand	Solvent	Ee (%)
1	**28a**	(***R***)-**31a**	CH_2Cl_2	50 (*S*)
2	**32**	(***R***)-**31b**	CH_2Cl_2	52 (*S*)
3[b]	**28a**	(***S***)-**33**	CH_2Cl_2	95 (*R*)
4	**32**	(***R***)-**31b**	EtOAc	24 (*S*)
5[b]	**28a**	(***S***)-**33**	EtOAc	93 (*R*)
6	**32**	(***R***)-**31a**	CH_2Cl_2	67 (*R*)
7	**32**	(***R***)-**31b**	CH_2Cl_2	80 (*R*)
8[b]	**32**	(***S***)-**33**	CH_2Cl_2	87 (*S*)

[a] Substrate (1 mmol), solvent (13 mL) under H_2 atmosphere, catalyst (0.01 mmol) $Rh(COD)_2BF_4$:ligand 1:2, 1 atm H_2, 25 °C, stopped after 100% conversion.

[b] Substrate (0.2 mmol, 0.04 M), catalyst (0.01 mmol) $Rh(COD)_2BF_4$: ligand 1:2, 1 atm H_2, 25 °C, 20 h, 100% conversion, Ref. [20].

4. Ferrocene-containing ligands

The ferrocenyl backbone is a widely used motif in asymmetric catalysis. It possesses a number of attractive properties which lead to its being the scaffold of choice for many metal complexes and their reactions. The ferrocenyl ring system provides a rigid and somewhat bulky backbone that is necessary for the induction of high stereoselectivity in many asymmetric metal-catalysed transformations and it is also particularly amenable to electrophilic substitution as a means of introducing donor atoms. 1,2-Disubstitution of one of the ferrocenyl rings with two different groups confers planar chirality on the system, which may augment central chirality of the substituents.

Van Leeuwen and co-workers prepared the C_2-symmetric bidentate ferrocenyl based ligands **36**, which possess central chirality at the phosphorus donor atom, Scheme 6 [21,22]. Steric and electronic variations were introduced by altering the substitution pattern on the coordinating phosphorus atoms and on the ferrocenyl backbone. The electronically different series of ligands, for which steric bulk was kept constant, were applied in the Pd-catalysed allylic alkylation of 1,3-diphenylprop-2-enyl acetate with dimethyl malonate. There was, however, only a slight adverse effect on the enantioselectivity induced by the presence of the electron-withdrawing trifluoromethyl substituents (from 68% with **36a** to 61% and 63% with **36c** and **36d**, respectively). The more electron-donating *para*-methoxy groups had no real effect on results compared to the unsubstituted ligand **36a**.

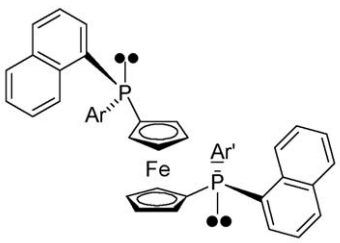

(S_p,S_p)-**36**

a Ar = Ar' = C_6H_5
b Ar = Ar' = 4-$MeOC_6H_4$
c Ar = Ar' = 4-$CF_3C_6H_4$
d Ar = 4-$MeOC_6H_4$; Ar' = 4-$CF_3C_6H_4$

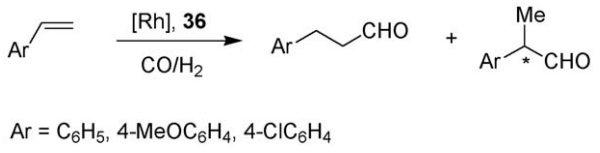

Scheme 18.

The employment of ligands **36a–d** in the asymmetric Rh-catalysed hydroformylation of styrene, *para*-methoxystyrene and *para*-chlorostyrene, was also investigated, Scheme 18 [23].

The selectivity-determining step is believed to involve trigonal-bipyramidal Rh intermediates in which the ligand can be coordinated in a bis-equatorial or equatorial-apical mode. As regards the optical induction of the process, bis-equatorial (ee) coordination by C_2-symmetric ligands could be considered more favourable than equatorial-apical (ea) binding since, by virtue of their being only one equatorial site available for substrate attachment and hydride migratory insertion, the number of diastereomeric species present is reduced, Fig. 3.

The bite-angle of approximately 100° for ferrocenyl ligands **36a–d** favours bis-equatorial complexation. High-pressure NMR and IR measurements were used to examine the effect of altering the electronics of the ligand on the coordination mode in the trigonal-bipyramidal complexes and to explore the subsequent influence on enantioselectivity. Both spectroscopic techniques indicated that the ee:ea equilibrium distribution was dependent on ligand basicity with the highest ratio being obtained for complexes derived from the least basic ligand **36c**. The electronic effect imposed by the *para*-methoxy group of ligand **36b** was found to be rather slight and the unsymmetrically substituted **36d** had an ee:ea ratio distinctly below those of either of the C_2-symmetric diphosphines.

Examination of the results of the rhodium-catalysed hydroformylation of styrene using ligands **36a–d** revealed low reactivities and regioselectivities perhaps due to steric reasons. Enantioselectivities were moderate in the best of cases and as predicted from the ee:ea ratios, the differences between the performances of the unsubstituted and the *para*-methoxy substituted ligands were minimal. The turnover frequency doubled on changing to the most electron-deficient *para*-trifluoromethyl ligand and enantioselectivity rose slightly to 50%. In accordance with the higher population of the ea coordination mode leading to lower enantioselection, the C_1-symmetric ligand **36d** gave the lowest value of 41%.

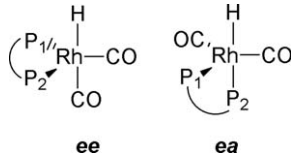

Fig. 3. Trigonal-bipyramidal Rh intermediates in hydroformylation.

Monitoring the hydroformylation of *para*-methoxystyrene and *para*-chlorostyrene led to the conclusion that ligand electronic effects did not have as great an influence on the reaction progress or outcome as did substrate electronic perturbations. However, for a given substrate, it was found that the reaction rate and amount of linear product were higher for the more electron-poor ligands. The optical induction on changing substrate did not follow a discernible trend, which demonstrated the ability of substrate electronic effects to overshadow those of the ligand.

Monodentate ferrocenyl phosphine ligands and their application in palladium-catalysed hydrosilylation of styrene, Scheme 19, with extremely high turnover frequencies have been reported by Johannsen and Pedersen [24]. The ligands **37a–e**, which they have termed aryl-MOPF ligands, possess planar chirality and in some cases where the aryl group is appropriately substituted, rotation about the ferrocene–aryl bond is restricted leading to similarities to conventional biarylic systems.

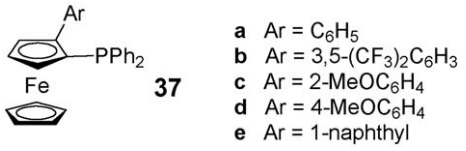

The results indicated that relatively electron-rich aryl substituents produced the highest reaction rates, but comparing entries 3 and 4 concerning *ortho*- and *para*-methoxy-Ph-MOPF, demonstrate that electronics are not the only influence on the reactivity, Table 16. Use of the electron-poor ligand **37b** resulted in a markedly slower rate to full conversion of the organosilane and a substantially lower ee of 25%. Although there appeared to be no direct relation between the steric and electronic properties of the ligand and the enantioselectivities obtained, the proposition put forward by Johannsen and Pedersen was that the combination of an electron-rich aryl substituent with steric flexibility is beneficial for high enantioselectivities.

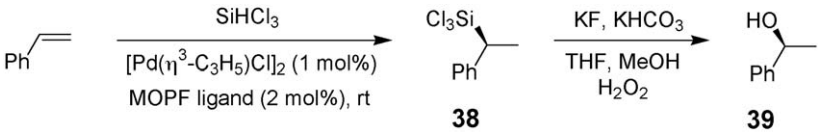

Scheme 19.

Table 16
Pd-catalysed hydrosilylation of styrene

Entry	Ligand	Time (h)	Conv.[a] to 38 (%)	Ee[b] of 39 (%)
1	**37a**	1.5	100	76
2	**37b**	8	100	25
3	**37c**	0.5	100	68
4	**37d**	1.6	100	86
5	**37e**	1.5	100	79

[a] Determined by HPLC.
[b] Determined by chiral HPLC.

Zheng and co-workers reported the synthesis of a series of new ferrocenylphosphine-imine ligands **39** and their subsequent application in palladium-catalysed allylic alkylation of 1,3-diphenylprop-2-enyl acetate [25].

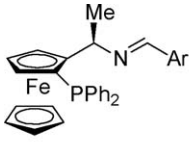

39

a Ar = C_6H_5 **b** Ar = 4-MeC_6H_4
c Ar = 4-$MeOC_6H_4$ **d** Ar = 4-$NMe_2C_6H_4$
e Ar = 4-ClC_6H_4 **f** Ar = 4-$NO_2C_6H_4$
g Ar = 2-$NO_2C_6H_4$ **h** Ar = 3-$NO_2C_6H_4$
i Ar = 3-$MeOC_6H_4$ **j** Ar = 3-ClC_6H_4

Ligands bearing electron-withdrawing substituents gave higher enantioselectivities than those containing electron-donating substituents, Table 17, entries 5,6,8–10. The position of the substituent on the phenyl ring was also found to be important with the *meta*-nitro-substituted **39h** providing a significant increase in ee and yield compared to the *para*-substituted analogue, entry 8 versus 6. The same was true for the chloro- and methoxy-containing ligands (compare entries 10 with 5 and 9 with 3) demonstrating the cooperativity that can be attained between steric and electronic influences.

Togni et al. witnessed strong electronic effects in the rhodium-catalysed hydroboration of styrene with the bidentate ferrocenyl-pyrazole family of ligands **40a–j**, wherein the electronics of both the pyrazole unit and the phosphorus donor atom were systematically modified [26]. For variations on the pyrazole ring, a dramatic enhancement of enantioselectivity was apparent on changing from electron-withdrawing trifluoromethyl substituent to the electron-donating methyl groups (33.4–95.6%), Table 18, entries 3 versus 1. Substituent size was also deemed a relevant factor in the process, with a slight reduction in enantioselection and reversal of regioselectivity when isopropyl substituents were used in place of the methyl groups, entries 5 versus 1 (see Scheme 20).

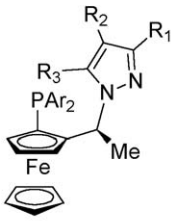

40

a R_1 = Me, R_2 = H, R_3 = Me, Ar = Ph
b R_1 = CF_3, R_2 = H, R_3 = CF_3, Ar = Ph
c R_1 = Me, R_2 = Me, R_3 = Me, Ar = Ph
d R_1 = CF_3, R_2 = H, R_3 =Me, Ar = Ph
e R_1 =*i*-Pr, R_2 = H, R_3 = *i*Pr, Ar = Ph
f R_1 = Me, R_2 = Br, R_3 = Me, Ar = Ph
g R_1 = H, R_2 = H, R_3 = H, Ar = Ph
h R_1 = Ph, R_2 = H, R_3 = Me, Ar = Ph
i R_1 = Me, R_2 = Br, R_3 = Me, Ar = Ph
j R_1 = Me, R_2 = NO_2, R_3 = Me, Ar = Ph
k R_1 = Me, R_2 = H, R_3 = Me, Ar =4-$CF_3C_6H_4$
l R_1 = Me, R_2 = H, R_3 = Me, Ar =4-$MeOC_6H_4$

Table 17
Pd-catalysed allylic alkylation of 1,3-diphenylprop-2-enyl acetate

Entry[a]	Ligand	Yield[b] (%)	Ee[c] (%) (*S*)
1	**39a**	51	73
2	**39b**	59	83
3	**39c**	53	83
4	**39d**	56	84
5	**39e**	67	86
6	**39f**	91	87
7	**39g**	78	80
8	**39h**	99	93
9	**39i**	97	91
10	**39j**	96	90

[a] Reaction conditions: toluene, 2.0 mol% $[Pd(\eta^3\text{-}C_3H_5)Cl]_2$, 5.0 mol% ligand, 3.0 equiv. Dimethyl malonate, 3.0 equiv. BSA, catalytic amount KOAc, room temperature.
[b] Isolated yields.
[c] Determined by chiral HPLC.

Table 18
Rh-catalysed hydroboration of styrene

Entry[a]	Ligand	Regioselectivity α:β	Ee (%) (*R*)	Yield (%)
1	**40a**	66:34	95.1	91
2	**40b**	61:39	33.4	78
3	**40c**	79:21	95.6	90
4	**40d**	46:54	43.8	79
5	**40e**	36:64	91.6	55
6	**40f**	65:35	95.7	80
7	**40g**	41:59	65.2	71
8	**40h**	47:53	79.6	92
9	**40i**	–	95.5	–
10	**40j**	–	84	–
11	**40k**	60:40	98.5	68
12	**40l**	61:39	90.0	61

[a] For entries 9 and 10, see Ref. [27], for all other entries, see Ref. [26].

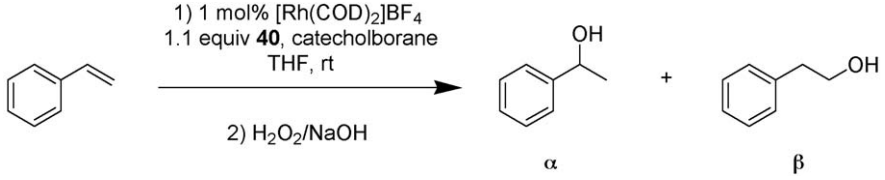

Scheme 20.

When the electron-rich pyrazole unit was maintained and the electronic nature of the phosphorus atom was varied, the highest ee to date for the Rh-catalysed hydroboration of styrene (98.5%) was achieved using ligand **40k** bearing electron-withdrawing trifluoromethyl substituents, entry 11 [27]. Electron-donating groups on the aryl rings reduced the enantioselectivity relative to the unsubstituted case, entries 12 versus 1. Thus the tentative conclusion was made that the combination of an electron-rich pyrazole component (good σ-donor, poor π-acceptor) and an electron-poor phosphine group (good π-acceptor) maximised the electronic asymmetry necessary for high enantioselective induction. However, notable exceptions were encountered by placing the electron-withdrawing Br or NO_2 substituents in the 4 position of the pyrazole ring, which resulted in anomalously high enantiomeric excesses of 95.5% and 84%, respectively, entries 9, 10. The implication was made that substituents at this position did not influence the course of the reaction solely by affecting the donor ability of the pyrazole nitrogen.

The relative electronic influences of the ligands were also evaluated by examining the carbonyl IR stretching frequencies of the Rh(CO)ligand complexes derived from **40a**–**l**, in which the CO group is *trans* to the pyrazole unit and therefore *cis* to the phosphorus of the ligand, Scheme 8. The observed trend in enantioselectivity was reflected in the CO stretching frequencies recorded, whereby a lower *ν*(CO) caused by a *trans* σ-donating pyrazole or a higher *ν*(CO) caused by a *cis* π-accepting phosphorus is accompanied by an increase in enantioselectivity for the Rh-catalysed hydroboration of styrene (see Scheme 21).

Togni acknowledged that making the pyrazole nitrogen donor less electron-rich might cause its partial dissociation from the metal centre and that this, rather than pure electronic effects could be the significant factor leading to the lower enantiomeric excesses such as the 33.4% obtained using the trifluoromethyl-substituted ligand **40k**. Therefore, ^{1}H and ^{31}P NMR studies were performed on [Rh(1,5-COD)(ligand)]BF_4 complexes but no partial ligand dissociation was observed. The addition of less than one equivalent of PEt_3 or PPh_3 resulted in quantitative incorporation of the additive to form [Rh(1,5-COD)$(PR_3)_2$]BF_4 indicating that the ligands either dissociate completely or not at all. Likewise, the use of a large excess of styrene did not result in the detection of any partially decomplexed ligand-containing species and so it was concluded that such dissociation of the ligand from the catalytically active intermediate was not taking place and the results obtained were primarily reflecting electronic effects.

A series of electronically-varied bidentate ferrocene–oxazoline ligands **41** and **42** developed by Hou, Dai et al. have been shown to have a significant impact upon the regioselectivity of the intermolecular Heck reaction [28,29].

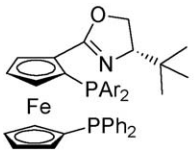

41

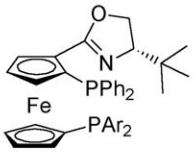

42

a Ar = C_6H_5
b Ar = 3,5-$(CF_3)_2C_6H_3$
d Ar = 3,5-$Me_2C_6H_3$
f Ar = 4-$CF_3C_6H_4$
h Ar = 4-$MeOC_6H_4$

c Ar = 3,5-$(CF_3)_2C_6H_3$
e Ar = 3,5-$Me_2C_6H_3$
g Ar = 4-$CF_3C_6H_4$
i Ar = 4-$MeOC_6H_4$

Two products **43** and **44** can emerge from the Heck reaction due to the possibility of double-bond migration, Scheme 22. The product distribution obtained is dependent on a number of variables such as solvent, base, Pd source and ligand.

The generally accepted mechanism for the Pd-catalysed asymmetric Heck reaction involves the formation and subsequent reaction of the hydride-olefin complex **45**, Scheme 23. Dai and Hou suggested that product **43** is generated from complex **45** via an 18-electron transition state formed by nucleophilic attack at the metal. When $Pd(OAc)_2$ served as the palladium source, the acetate anions caused this nucleophilic displacement to give **43**. However, if $Pd(dba)_3 \cdot dba$ was used, there was no such nucleophile and so palladium could re-insert into the double bond yielding complex **46** which, following β-hydride elimination and dissociation, gave product **44**. This prompted Dai and co-workers to synthesise an electronic series of their ferrocene–oxazoline ligands **41** and **42** in an attempt to alter the

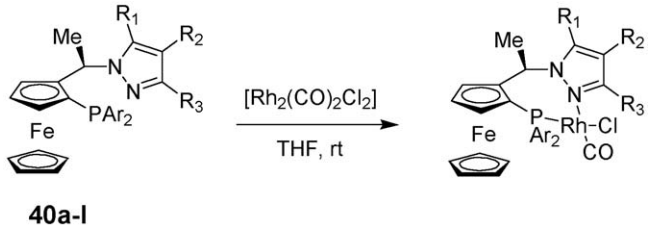

40a-l

Scheme 21.

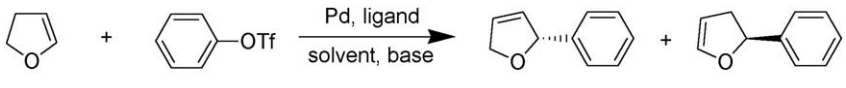

43 **44**

Scheme 22.

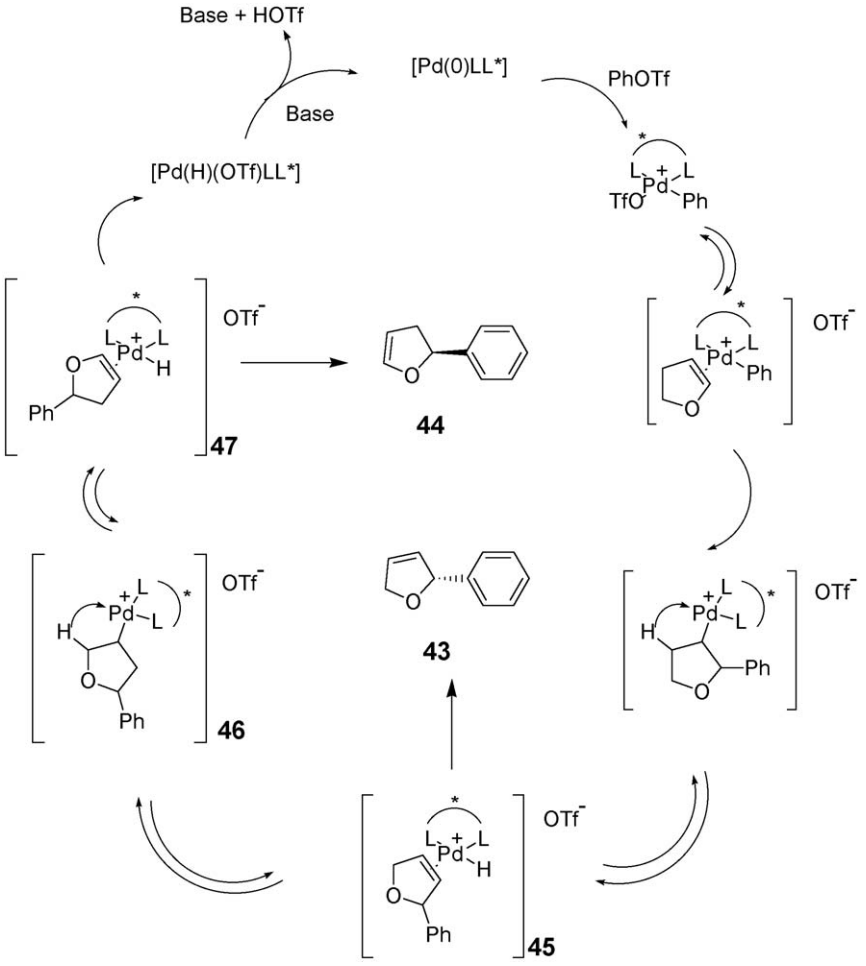

Scheme 23.

electrophilicity of the palladium centre, thereby enhancing the **43**:**44** product ratio.

A pronounced difference in regioselectivity was noted between the reactions involving the electron-deficient 3,5-$(CF_3)_2C_6H_3$- and the electron-rich 4-$MeOC_6H_4$-substituted ligands **42c** and **42i**, Table 19, entries 1 versus 5. This was attributed to a reduction in the electron density at Pd in hydride-olefin complex **45** derived using ligand **42c** further influencing nucleophilic attack leading to an increased production of product **43**. In contrast, a more electron-donating ligand such as **42i** increases the electron density at palladium, allowing for re-insertion into the olefin and eventual formation of isomer **44**.

Introducing the same electronic differences into the upper cyclopentadienyl ring containing the oxazoline substituent did not result in such a marked change in the

Table 19
Pd-cataylsed intermolecular Heck reaction

Entry[a]	Ligand	Pd source	Solvent	Conv.[b] (%)	Ratio 43:44[b]	Ee[c] (%) 43 (*R*)	Ee[c] (%) 44 (*S*)
1	**42c**	$Pd(OAc)_2$	Toluene	67	99:1	92	nd
2	**42c**	$Pd(dba)_3 \cdot dba$	THF	86	89:11	94	20
3	**42e**	$Pd(OAc)_2$	Toluene	73	93:7	96	nd
4	**42g**	$Pd(OAc)_2$	Toluene	80	64:36	83	29
5	**42i**	$Pd(OAc)_2$	Toluene	65	14:86	86	27
6	**42i**	$Pd(dba)_3 \cdot dba$	THF	100	15:85	94	48
7	**41b**	$Pd(OAc)_2$	Toluene	72	94:6	75	13
8	**41d**	$Pd(OAc)_2$	Toluene	77	90:10	98	nd
9	**41f**	$Pd(OAc)_2$	Toluene	98	95:5	97	29
10	**41h**	$Pd(OAc)_2$	Toluene	67	83:17	98	29

[a] 1.5 mol% palladium precursor, 3 mol% ligand, iPr_2NEt base, 60 °C, 36 h.
[b] Determined by GC.
[c] Determined by chiral GC; nd = not determined.

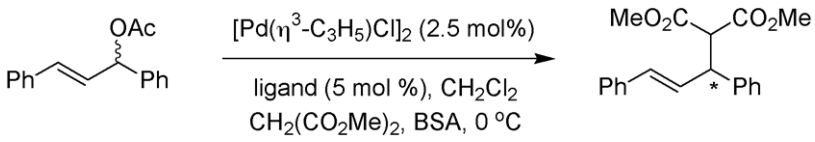

Scheme 24.

product distribution, entries 7–10. This was believed to be due to the oxazoline group acting as an electron-withdrawing species, which swamps the effect of additional electronic variations on the upper Cp ring. The electronic effects were further investigated through the application of the DPPF analogues **48** and **49**. Again, a reversal in the regioselectivity was observed on changing the electronic nature of the phosphorus aryl groups.

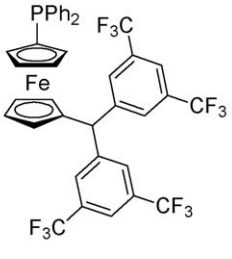

48

72 h, 71 % conv., 61:39 **43**:**44**

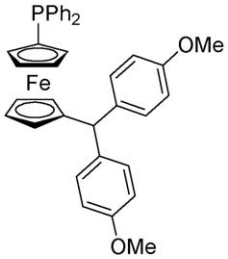

49

96 h, 100 % conv., 9:91 **43**:**44**

The diphosphine ligands **41** and **42** were also used to introduce electronic asymmetry in the palladium-catalysed allylic alkylation of 1,3-diphenylprop-2-enyl acetate, Scheme 24 [30]. All the ligands screened provided highly active catalysts with quantitative yield obtained in almost all cases within 1 h at 0 °C. Electron-withdrawing ligands induced the highest enantiomeric excesses, Table 20, entries 2,3 and 7, while the use of electron-donating ligands resulted in less selective reactions, entries 4,8 and 9. In a further assessment of the influence of ligand electronics on the enantioselective outcome, use of the strongly electron-donating ligands **50** and **51**, wherein the phenyl groups on the top and bottom Cp rings, respectively, were replaced with cyclohexyl rings, yielded almost racemic product, entries 10 and 11.

Table 20
Pd-catalysed allylic alkylation of 1,3-diphenylprop-2-enyl acetate

Entry	Ligand	Time (h)	Yield (%)[a]	Ee[b] (%) (*S*)
1	**41a**	0.75	98	81.6
2	**41b**	1	99	90.1
3	**42c**	1	99	84.3
4	**41d**	0.5	99	75.1
5	**42e**	1	99	83.5
6	**41f**	1	99	82.3
7	**42g**	1	99	84.3
8	**41h**	1	98	69.2
9	**42i**	0.5	100	70
10	**50**	24	90	5.2
11	**51**	1	98	8.6
12	**52**	<0.5	100	91.5

[a] Isolated yield.
[b] Determined by chiral HPLC.

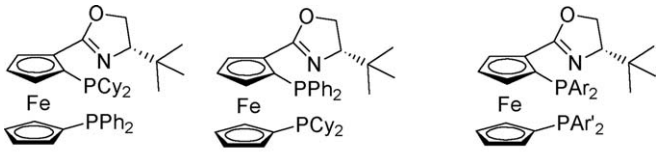

50 **51** **52**

In order to rationalise the observed electronic effects, the key (π-allyl)(ligand)Pd intermediate of the allylic alkylation reaction was considered. The researchers assumed that the M-type configuration was more favourable due to the steric repulsion between the allyl phenyl ring and the oxazoline unit of the ligand. Nucleophilic attack would occur at the allyl terminus *trans* to the more electron-deficient phosphorus and when this coincided with the steric influence of the oxazoline ring (attack *trans* to the oxazoline ring is preferable) high enantiomeric excesses of the *S* product would result from use of the *S* ligand. This explained the 90% ee obtained using ligand **41b**, where the more electron-deficient phosphorus was located on the oxazoline-containing Cp ring, entry 2. On the other hand, when the electron density of the phosphorus atom on the lower Cp ring was lower than that of the upper ring, nucleophilic attack at the opposite allyl terminus becomes easier which does not match the steric influence of the oxazoline ring and so lower enantiomeric excesses are seen, entry 8.

In an attempt to benefit from these implications, ligand **52**, containing an electron-poor phosphorus on the upper Cp ring and an electron-rich phosphorus on the lower ring, was prepared. However, its application in the allylic alkylation reaction resulted in only a slightly enhanced enantioselectivity of 91.5%, entry 12.

5. Oxazoline- and imidazoline-containing ligands

An early example of the application of electronically-variable ligands incorporating oxazolines was that of the Pybox derivatives **53** by the group of Nishiyama in 1992 [31]. Rhodium-complexes of the ligands were screened in the hydrosilylation of acetophenone to determine the effect

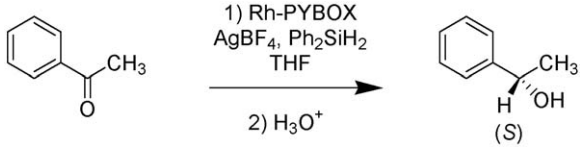

Scheme 25.

of altering the basicity of the pyridyl nitrogen on the reaction outcome, Scheme 25.

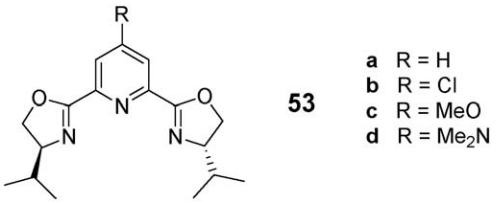

53

a R = H
b R = Cl
c R = MeO
d R = Me_2N

They reported that the substituent on the pyridyl group influenced the critical temperature necessary for the reaction to progress smoothly, i.e. ligands possessing electron-rich substituents required higher reaction temperatures and longer times to give a high yield, Table 21, entries 1–4.

Table 21
Rh-catalysed hydrosilylation of acetophenone

Entry	Ligand	Temperature (°C)	Time (h)	TON	Yield (%)	Ee (%) (*S*)
1	**53a**[a]	0	6	100	86	83
2	**53b**[a]	−5	3	100	94	83
3	**53c**[a]	10	3	100	89	89
4	**53d**[a]	20	6	100	78	92
5	**53a**[b]	20	1	128	64	43
6	**53b**[b]	20	1	154	77	2
7	**53c**[b]	20	1	85	42	58
8	**53d**[b]	20	1	43	22	59

[a] Acetophenone (8.0 mmol), Ph_2SiH_2 (12.8 mmol), $AgBF_4$ (0.16 mmol), THF (1 mL).
[b] Acetophenone (16.0 mmol), Ph_2SiH_2 (25.6 mmol), $AgBF_4$ (0.16 mmol), THF (2 mL).

Additionally, ligand activity was compared by performing each reaction at 20 °C for 1 h. In this set of experiments, the same trend was noted with the turnover number being greatest for the less basic *para*-chloro-substituted ligand **53b**, entry 6. However, for this ligand, increasing the reaction temperature from −5 °C to 20 °C caused a drop in the enantioselectivity from 83% to 2%, entry 2 versus 6. This suggested that the catalyst decomposed at higher temperatures, generating achiral rhodium species that served to promote the reaction without any selectivity. The use of electron-donating pyridine substituents improved the enantioselectivity relative to the unsubstituted ligand, entries 7 and 8 versus 6. Similar effects on the reaction rates were observed for the hydrosilylation of α-tetralone and 2-phenylethyl methyl ketone. The influence of the electronic nature of the ligand on reaction rate was attributed to its effect on the stability of the rhodium species from which the final product is dissociated. Electron-rich ligands were thought to enhance the stability of the complex and hence reduce the turnover number, whereas electron-deficient ligands produced the opposite effect.

The same family of ligands was also screened in the ruthenium-catalysed cyclopropanation of styrene with ethyl diazoacetate, Scheme 26, Table 22 [32].

The use of electron-rich pyridyl units adversely affected both the catalytic activity and enantioselectivity of the reaction, although the *trans*:*cis* selectivity was consistent at around 90:10 throughout the series. The dimethylamino-substituted ligand produced virtually no activity, entry 1, whereas the relatively electron-deficient ligands

Table 22
Ru-catalysed cyclopropanation of styrene

Entry	Catalyst	Temperature (°C)	Yield (%)	*Trans*:*cis*	Ee (%) *trans*, *cis*
1	**54a**	25	2	88:12	80, 53
2	**54b**	25	29	92:8	86, 70
3	**54c**	25	73	91:9	89, 79
4	**54d**	25	60	92:8	90, 80
5	**54e**	25	74	91:9	93, 87

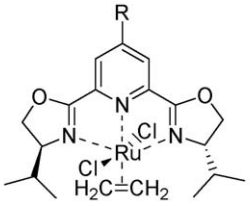

54

a $R = NMe_2$
b R = OMe
c R = H
d R = Cl
e $R = CO_2Me$

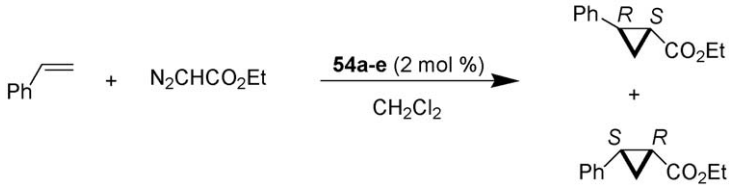

Scheme 26.

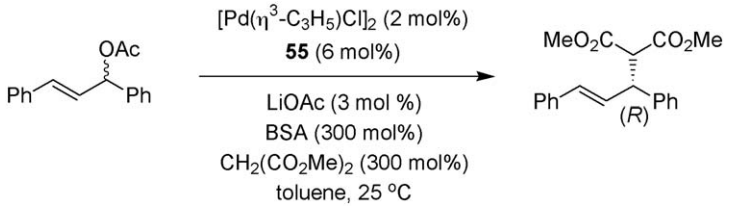

Scheme 27.

gave yields of up to 74%, entries 3–5. Enantioselectivities were also higher with electron-withdrawing analogues, entry 5 versus 1. The improved results observed for the electron-poor Pybox ligands was believed to be due to their increasing the reactivity of the intermediate Ru-carbene complex towards the olefin, with the opposite being true for electron-rich ligands.

An unusual class of electronically-tunable oxazoline-containing ligands **55a–d** have recently been introduced by Hou et al. [33]. The phosphine basicity of these planar chiral *P*,*N*-[2.2]paracyclophane ligands was altered through substitution of the aryl groups and the resulting ligands were tested in the palladium-catalysed allylic alkylation of 1,3-diphenylprop-2-enyl actetate, Scheme 27. In comparison to the *para*-methyl-substituted ligand **55b**, the more electron-rich *para*-methoxy analogue **55c**, proved superior by inducing a greater enantioselectivity and a faster reaction rate, Table 23, entries 2 versus 3. Accordingly, application of the electron-deficient, trifluoromethyl-substituted ligand **55d** necessitated a longer reaction time to reach the same conversion and the ee was significantly reduced, entry 4.

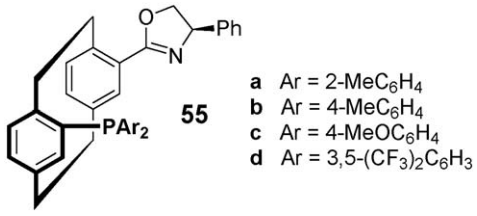

Table 23
Pd-catalysed allylic alkylation of 1,3-diphenylprop-2-enyl acetate

Entry	Ligand	Time (min)	Yield (%)[a]	Ee (%)[b]
1	**55a**	180	98	6
2	**55b**	60	98	69
3	**55c**	20	98	90
4	**55d**	240	98	49

[a] Isolated yield after flash chromatography.
[b] Determined by chiral HPLC.

Helmchen utilised substituted phosphinooxazolines **56** for the iridium-catalysed alkylation of monosubstituted allylic acetates, Scheme 28 [34]. Reaction with the parent ligand was relatively slow and unselective, Table 24, entry 1, whereas introducing the electron-withdrawing *para*-trifluoromethyl variant proved beneficial, with an ee of 91% being reported, entry 2. The inclusion of an additional CF_3 group caused the selectivity to decrease indicating that the steric bulk of the ligand is also a relevant factor.

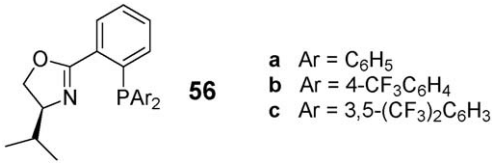

Imidazoline analogues of the PHOX ligands have been prepared by Pfaltz and co-workers [35] and by Busacca at Boehringer-Ingelheim Pharmaceuticals [36]. Further electronic and steric tuning relative to the oxazoline ligands is possible due to the presence of the additional nitrogen atom of the imidazoline unit. For the iridium-catalysed hydrogenation of a range of unfunctionalised olefins **60**, Pflatz focused the electronic modifications on the amine nitrogen of the imidazoline ring of ligands **61**,

Table 24
Ir-catalysed alkylation of monosubstituted allylic acetates

Entry	Substrate	Ligand	Yield (%)	Ratio of **58**:**59**	Ee of **58** (%) (*R*)
1	**57a**	**56a**	61	92:8	30
2	**57a**	**56b**	99	95:5	91
3	**57a**	**56c**	95	89:11	84
4	**57b**	**56a**	89	99:1	72
5	**57b**	**56b**	98	99:1	95
6	**57b**	**56c**	71	93:7	62

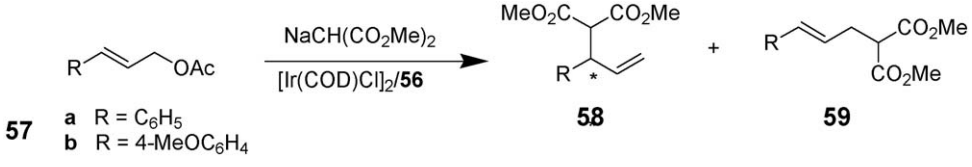

Scheme 28.

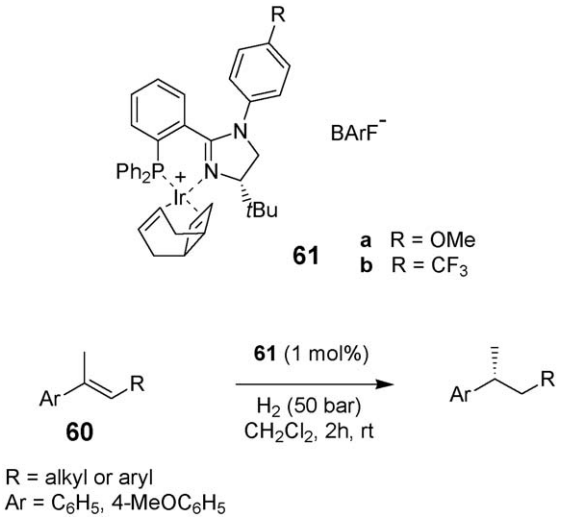

Scheme 29.

Scheme 29 but did not find a significant deviation in enantioselectivity or conversion relative to the electronically-neutral case.

Busacca screened a more extensive range of the ligand series in the asymmetric Heck reaction to form oxindoles, Scheme 30. The initial results obtained indicated that electron-donating and electron-withdrawing groups on the imidazoline nitrogen gave the opposite enantiomer of product. The Hammett plot of log er (enantiomer ratio) versus σ_p of the *N*-benzoyl *para* substituent showed a random distribution and the enantioselectivities spanned a fairly small range of 33–48% and so it was inferred that this position was too far from the metal centre to greatly affect the enantioselectivity. Varying the substitution of the phosphine groups while maintaining the 2-naphthoyl substituent on nitrogen, gave a more satisfying Hammett plot displaying a linear relationship between the electronic constant and enantioselectivity. The enantiomeric excesses covered a broader range (40–78%) and the best result for this substrate was obtained using 3,5-difluorophenyl substituents.

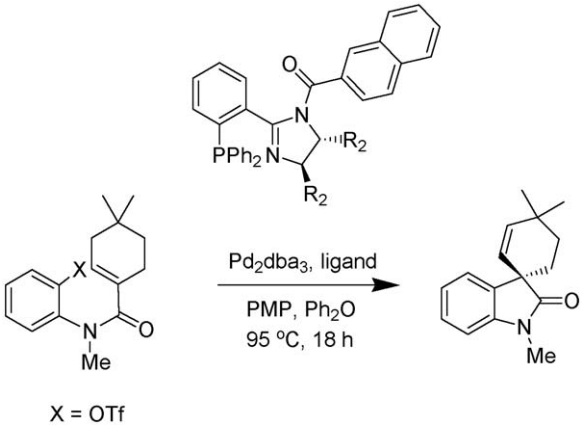

Scheme 30.

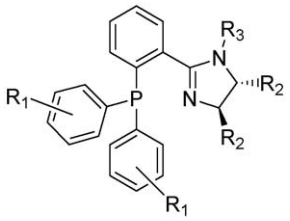

The effect of manipulating the electronics at the imidazoline carbons was also examined. In general, higher enantioselectivities were obtained using less basic ligands, Table 25, compare entries 8 and 7, 6 and 2. Since any substitution led to an increase in ee compared to the unsubstituted case, entry 3, and the fact that *para*-substitution severely hampered the reaction progress whereas increased yields were obtained for 3,5-disubstituted components, steric control also plays an important role in the reaction.

In the final ligand optimisation studies, the substituents at each location leading to the highest enantiomeric excesses were combined to produce considerably electron-poor ligands, Table 26. This resulted in low turnovers when PMP was used as base but the yield was improved by instead employing cyclohexylethyl pyrrolidine with no reduction in enantioselectivity. The optimal ligand for the chosen substrate was thus deemed to be **62**, where $R_1 = 3,5\text{-}F_2$ and $R_3 = 2$-naphthoyl, delivering the product in 88% ee as compared to 46% obtained using the PHOX ligand.

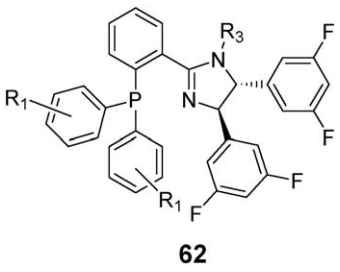

Table 25
Pd-catalysed intramolecular Heck reaction

Entry[a]	R_2	Yield[b] (%)	Ee[c] (%)
1	(*S*,*S*)-4-$MeOC_6H_4$	13	51.6 (+)
2	(*R*,*R*)-4-MeC_6H_4	25	45.2 (−)
3	(*S*,*S*)-C_6H_5	68	44.6 (+)
4	(*S*,*S*)-4-FC_6H_4	61	48.3 (+)
5	(*S*,*S*)-4-ClC_6H_4	17	61.5 (+)
6	(*R*,*R*)-4-$CF_3C_6H_4$	12	64.6 (−)
7	(*S*,*S*)-3,5-$Me_2C_6H_3$	85	46.7 (+)
8	(*S*,*S*)-3,5-$F_2C_6H_3$	93	62.7 (+)

[a] All reactions in Ph_2O with PMP as base.
[b] Isolated yield after 18 h.
[c] Determined by chiral HPLC, sign of rotation of major enantiomer.

Table 26
Pd-catalysed intramolecular Heck reaction

Entry[a]	R_1	R_3	Yield[b] (%)	Ee[c] (%)
1	4-Cl	2-Naphthoyl	25	80.6 (−)
2	4-Cl	2-Naphthoyl	51[c]	79.3 (−)
3	4-Cl	4-MeOBz	28	78.2 (−)
4	4-Cl	4-CF_3Bz	26	74.9 (−)
5	3,5-F_2	2-Naphthoyl	50[c]	86.8 (−)
6	3,5-F_2	2-Naphthoyl	38	87.6 (−)

[a] Reactions in Ph_2O with PMP base unless otherwise stated.
[b] Determined by chiral HPLC.
[c] 1-(1-Cyclohexylethyl)-pyrrolidine as base.

6. Diphosphine and phosphinamine ligands

Chiral diphosphines based on the 2,4-pentane-2,4-diyl backbone have been used extensively in asymmetric catalysis. Electronic tuning of such bis(diphenylphosphino)pentane ligands was reported by Bakos et al. in 2004 [37]. They varied the substitution pattern of the aryl groups to modify the donor phosphine basicity and applied rhodium complexes of the resulting ligands in the asymmetric hydrogenation of (*Z*)-α-acetamidocinnamic acids and esters, Scheme 31.

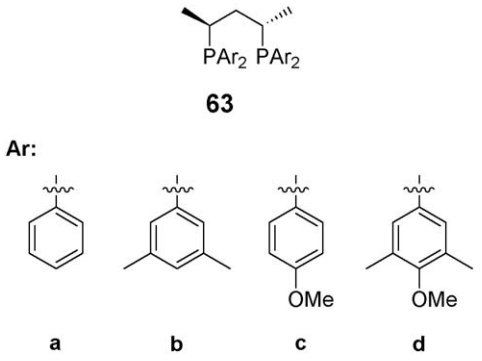

The results indicated that for dimethyl itaconate higher catalytic activity and enantioselectivity was seen for less electron-rich phosphines, Table 27, entries 1–4. When more electron-rich substrates were used, enantioselectivies were much improved and in contrast to the hydrogenation of dimethyl itaconate, selectivity and activity were greater

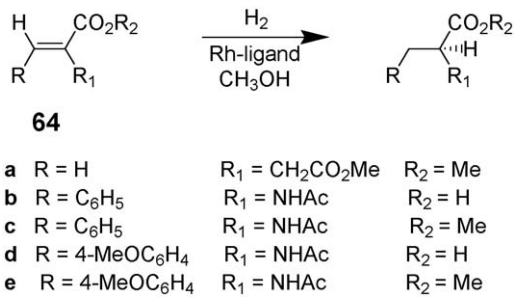

Scheme 31.

Table 27
Rh-catalysed hydrogenation of (*Z*)-α-acetamidocinnamates

Entry[a]	Ligand	Substrate	S/C	Time (min)	Conv. (%)	Ee (%)[b] (*R*)
1	**63a**	**64a**	500	5	100	63.1
2	**63b**	**64a**	500	5	100	49.4
3	**63c**	**64a**	500	22	95	32.8
4	**63d**	**64a**	500	45	77	8.4
5	**63a**	**64b**	50	8	100	94.4
6	**63b**	**64b**	50	2	100	97.2
7	**63b**	**64b**	200	3	100	96.9
8	**63c**	**64b**	50	2	100	82.2
9	**63d**	**64b**	50	5	100	96.5
10	**63a**	**64c**	100	3	100	78.0
11	**63b**	**64c**	200	2	100	90.8
12	**63b**	**64d**	100	2	100	98.3
13	**63b**	**64e**	50	11	100	91.3

[a] Reaction conditions: entries 1–4, 23 °C, $p(H_2)$ 20 bar; entries 5–13, 15 °C, $p(H_2)$ 1 bar.
[b] Determined by chiral GC.

with electron-releasing ligands, entries 5 versus 6, 8 versus 7. Increasing the electronic nature of the substrate also resulted in an increase in ee, entries 12 versus 7 and 13 versus 11. This observed enhancement of enantioselectivity was attributed to a faster rate of oxidative addition of hydrogen to a more electron-rich metal centre accompanied by an increased rate of reaction of one of the major and minor diastereomeric substrate-containing rhodium complexes relative to the other. The fact that opposing trends in electronic requirements were noted for the itaconate substrate and the more electron-rich olefins was believed to be due to the involvement of different mechanistic pathways.

Casey and co-workers applied electronically dissymmetric diphosphines in the Rh-catalysed hydroformylation of 1-hexene [38]. Regioselectivity in hydroformylation is believed to be dependent on the coordination mode (i.e. bisequatorial, ee versus equatorial-apical, ea) of the ligands employed, Scheme 32.

Studies of the catalytic systems involving the ligands BISPI **65** and T-BDCP **66**, which exhibit bis-equatorial chelation, showed that the addition of electron-withdrawing aryl substituents led to an increase in the linear to branched ratio (l:b). However, introducing electron-withdrawing substituents on the aryl groups of DIPHOS **67**, which coordinates in an equatorial-apical fashion, resulted in a decrease in the l:b ratio [39]. This led to their hypothesis that an electron-withdrawing substituent on an equatorial phosphine increases the l:b ratio while an electron-withdrawing substituent on an apical phosphine has the opposite effect, Fig. 4.

To maximize this electronic influence with the hope of improving the regioselectivity, dissymmetric derivatives of DIPHOS **67a–d** were synthesised. ^1H and ^{31}P NMR studies of the corresponding [ligand]$Ir(CO)_2H$ species showed that all the complexes were a mixture of two equilibrating isomers. For ligands DIPHOS-(3,5-CF_3, H) and

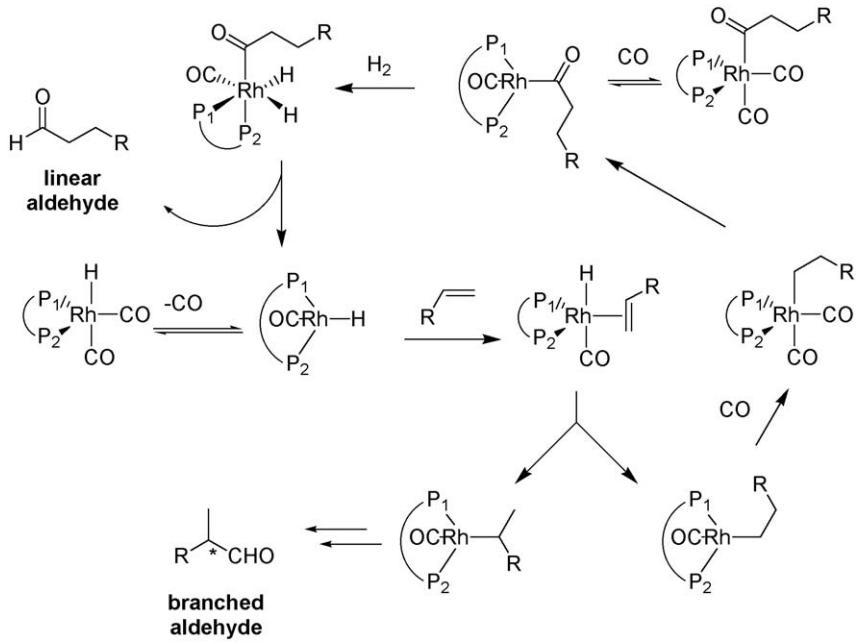

Scheme 32.

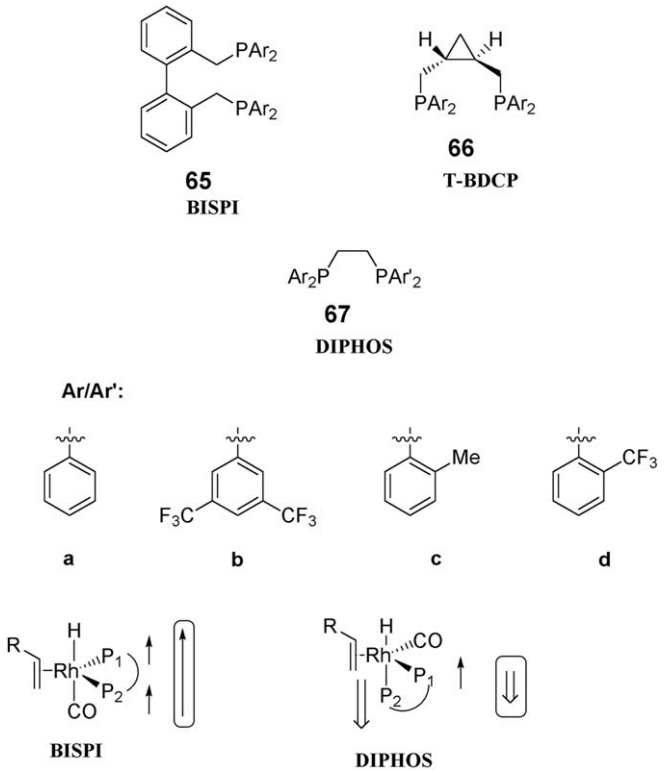

Fig. 4. Rh coordination modes with BISPI and DIPHOS.

DIPHOS-(3,5-CF_3, 2-Me), the major isomers have the electron-withdrawing phosphine in the equatorial position, (calculated diastereomeric ratios at room temperature of 83:17 and 88:12, respectively), which was the desired coordination mode for the testing of their hypothesis. For the 2-CF_3-substituted ligands, the ratio was not as pronounced but still lay in favour of positioning the electron-poor phosphine in the equatorial site, 65:35 and 68:32 for DIPHOS-(2-CF_3, H) and DIPHOS-(2-CF_3, 2-Me), respectively.

Results from the rhodium-catalysed hydroformylation of 1-hexene, Scheme 33, proved that the dissymmetric ligand DIPHOS-(3,5-CF_3, H) was indeed more regioselective than either of the two symmetrically substituted analogues, Table 28, entries 5 versus 1 and 2. This increase in l:b regioselectivity was accounted for by the predominance of the [ligand]Ir$(CO)_2$H diastereomer wherein the electron-deficient phosphine is located in the equatorial position, Fig. 5. Although the relative rates of reaction of the major and minor isomers were not determined, the similar reaction rates for the symmetrical counterparts suggested that two dissymmetric diastereomers react at comparable rates.

Increases in the product ratio were seen for the other three electronically dissymmetric ligands relative to the symmetrically substituted variants. The improvement was not as enhanced when ligands DIPHOS-(2-CF_3, H) and DIPHOS-(2-CF_3, 2-Me) were tested, entries 6 versus 1 and 4 and entries 8 versus 3 and 4, which was attributed

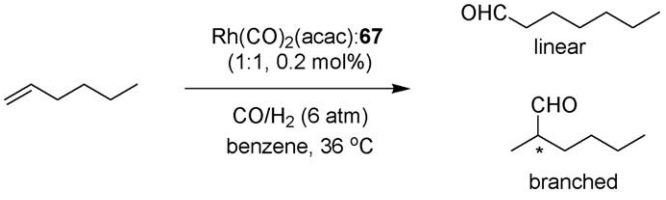

Scheme 33.

Table 28
Rh-catalysed hydroformylation of 1-hexene

Entry	Ligand	Ir complex ratio[a]	Aldehyde l:b ratio[b]	Regioselectivity% l	Turnover rate[c]
1	DIPHOS	100:0	2.6:1	71.9	3.5
2	DIPHOS-(3,5-CF_3)	100:0	1.3:1	56.9	4.3
3	DIPHOS-(2-Me)	100:0	3.0:1	75.2	4.0
4	DIPHOS-(2-CF_3)	100:0	2.6:1	72.1	0.4
5	DIPHOS-(3,5-CF_3,H)	83:17	4.2:1	80.8	2.5
6	DIPHOS-(2-CF_3,H)	65:35	2.9:1	74.1	3.8
7	DIPHOS-(3,5-CF_3,2-Me)	88:12	3.3:1	76.9	4.7
8	DIPHOS-(2-CF_3,2-Me)	68:32	3.8:1	79.1	2.7

[a] Ratio of ea-1:ea-2 isomers of (ligand)$Ir(CO)_2H$ at room temperature.
[b] Moles of heptanal:moles of 2-methylhexanal.
[c] Turnover rate = [moles aldehyde][moles Rh]$^{-1}$ h^{-1}.

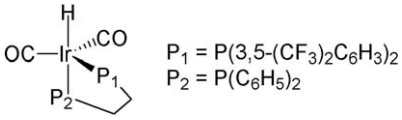

Fig. 5. Ir-diphosphine intermediate.

to the reduced ratio of major to minor iridium diastereomers.

Morimoto et al. reported the synthesis of the L-valine-derived P,N ligands **68a–f**, and their application in the palladium-catalysed allylic alkylation of 1,3-diphenyl-prop-2-enyl pivalate **69**, Scheme 34 [40].

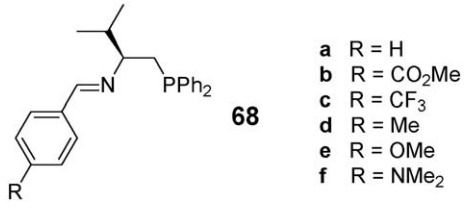

Varying the electronic nature of the substituent affected both the enantioselectivity and catalytic activity, whereby ligand **68f** containing the electron-releasing dimethylamino group provided the most active catalyst along with the highest ee of 92%, Table 29, entry 6. The catalyst loading could be further reduced with only a slight reduction in the enantioselectivity, entry 7. The application of ligands bearing electron-withdrawing substituents had a detrimental effect on both the conversion and enantioselectivity compared to the parent ligand, entries 2 and 3 versus 1.

Table 29
Pd-catalysed allylic alkylation of 1,3-diphenylprop-2-enyl acetate

Entry[a]	Ligand	R	Yield[b] (%)	Ee[c] (%)
1	**68a**	H	57	52
2	**68b**	CO_2Me	42	19
3	**68c**	CF_3	46	38
4	**68d**	Me	76	74
5	**68e**	OMe	88	85
6	**68f**	NMe_2	99	92
7[d]	**68f**	NMe_2	94	89

[a] Molar ratio: $[Pd(\eta^3\text{-}C_3H_5)Cl]_2$/ligand/substrate/dimethyl malonate/BSA/lithium acetate = 2.5/2–10/100/300/300/5.
[b] Isolated yield.
[c] Determined by chiral HPLC.
[d] 0.5 mol% $[Pd(\eta^3\text{-}C_3H_5)Cl]_2$.

The substantial difference between the performances of the trifluoromethyl- and the methyl-substituted ligands **68c** and **68d** demonstrates the strong electronic influence in the absence of a steric effect [41].

7. Axially chiral phosphines

A monophosphine BINAP analogue H-MOP **70a**, designed by Hayashi, was applied to the Pd-catalysed hydrosilylations of styrene derivatives, Scheme 35 [42]. The hydrosilylation of styrene proceeded in 93% ee but transformations of the more electron-rich substrates, *para*-methylstyrene and *para*-methoxystyrene, to the corresponding alcohols were less selective (89% and 61% ee, respectively). This led to the development of a series of H-MOP ligands **70b–g** containing electron-donating or electron-withdrawing substituents on the phenyl rings [43].

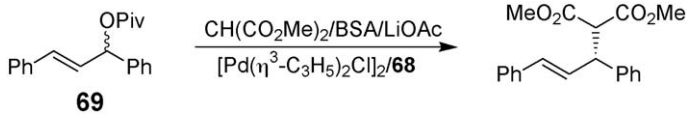

Scheme 34.

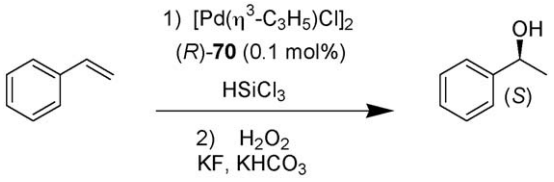

Scheme 35.

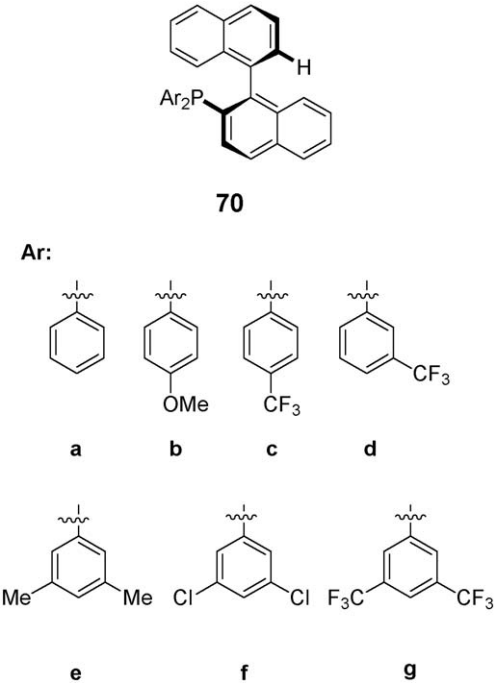

The results from the hydrosilylation of styrene revealed that electronic variations at the *para*-position of the phenyl groups did not have an effect on the enantioselectivity, Table 30, entries 2 and 3 versus 1. Improved enantioselection was obtained by placing an electron-withdrawing trifluoromethyl substituent in the *meta*-position, entry 4. Encouraged by this observation, further manipulation of the substitution pattern at the *meta*-positions was carried out, entries 5–8, whereupon the bis-trifluoromethyl-substituted analogue was found to deliver the highest ee of 97%, entry 7. Catalytic activity was also discovered to be best for this ligand, with almost full conversion obtained at 0 °C in 1 h as opposed to 12 h for the unsubstituted ligand, entry 7 versus 1. At −20 °C with ligand **70g**, the enantioselectivity was increased to 98%, which was the highest ee reported for the hydrosilylation of styrene.

para-Chlorostyrene, *para*-methylstyrene and *para*-methoxystyrene were also subjected to hydrosilylation catalysed by the Pd-complexes formed with **70g** and with its parent ligand **70a**, Scheme 36. High enantiomeric excesses were obtained for all substrates using ligand **70g** in contrast to the substantial difference between enantioselectivity induced by ligand **70a** when the electron-deficient *para*-chlorostyrene and electron-rich *para*-methoxystyrene were employed as substrates (94% versus 61% ee, respectively).

To gain insight into the mechanistic pathway and origin of the regioselectivity and enantioselectivity of the reaction, palladium-catalysed hydrosilylations of deuterated styrenes were examined [44]. It was concluded that with the electron-deficient ligand **70g**, β-hydride elimination from the alkylpalladium intermediate is fast compared to reductive elimination, whereas with ligand **70a**, β-hydride elimination does not proceed as quickly. The higher enantioselectivity achieved using ligand **70g** was therefore ascribed to fast β-hydride elimination which leads to rapid interconversion between the two possible diastereomeric intermediates *re*-**71** and *si*-**71**, Scheme 37, from which reductive elimination occurs at significantly different rates.

Thus, applying (*R*)-**70g**, *si*- and *re*-**71** are in fast equilibrium and reductive elimination from (*S*)-**72** gives the (*S*) product, whereas instead of reductive elimination, (*R*)-**72** favours β-hydride elimination followed by Pd-insertion ultimately leading towards (*S*) product. Since β-hydride elimination does not occur as fast using the unsubstituted ligand **70a**, there is greater opportunity for reductive elimination from (*R*)-**72** to take place, thereby reducing the

Table 30
Pd-cataylsed hydrosilylation of styrene

Entry[a]	Ligand	Temperature (°C)	Time (h)	Yield[b] (%)	Ee[c] (%) (*S*)
1	**70a**	0	12	100	93
2	**70b**	0	24	89	92
3	**70c**	0	11	92	93
4	**70d**	0	15	81	95
5	**70e**	0	16	95	92
6	**70f**	0	20	89	94
7[d]	**70g**	0	1	93	97
8	**70g**	−20	24	85	98

[a] Reactions carried out without solvent unless otherwise noted. Styrene:$HSiCl_3$:Pd:ligand 1:1.2:0.001:0.002.
[b] Isolated yield after distillation.
[c] Determined by chiral HPLCof (3,5dinitrophenyl)carbamate ester of alcohol product.
[d] In benzene (1.0 M solution).

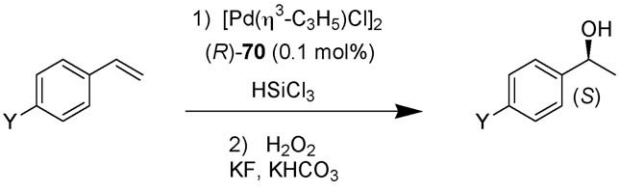

	70g	70a
Y = Cl	98 % ee	94 % ee
Y = Me	95 % ee	89 % ee
Y = OMe	97 % ee	61 % ee

Scheme 36.

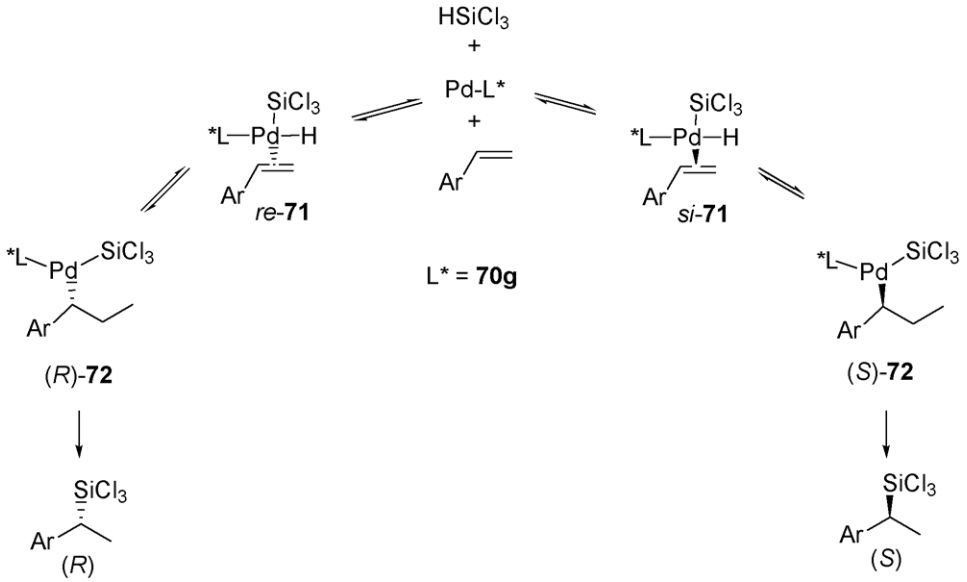

Scheme 37.

overall selectivity of the reaction. However, the studies did not provide information as to why the bis-trifluoromethyl ligand should cause faster β-hydride elimination than **70a** or if the influences were predominantly electronic or steric.

Axially chiral bidentate phosphine ligands have been used to provide extremely efficient catalysts for an extensive range of asymmetric transformations [45]. BINAP-derived ligands are among the most successful of these diphosphines. Impressive results had been obtained in asymmetric hydrogenation of olefins using mononuclear Ru-complexes but the same could not be said for the hydrogenation of ketones. Mashima and co-workers developed catalysts of the type [RuX(BINAP)(arene)]Y (X = halides, Y = anions), which promoted the asymmetric hydrogenation of both olefins and ketones [46]. They identified the importance of reaction conditions, the halide bound to Ru and phenyl-ring substitution patterns on the reaction outcome [47]. In a further investigation of the influence of the electronic and steric properties of the substituents on the phenyl rings of BINAP, the derivatives **73** were synthesised and applied in the hydrogenation of olefinic and ketonic substrates, Scheme 38 [48].

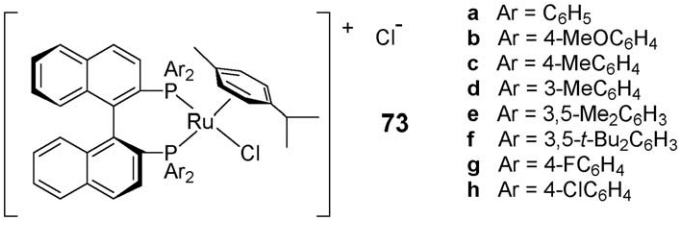

The results for the asymmetric hydrogenation of **74** showed that no remarkable changes in selectivity occurred when Ru(II) complexes of the methyl- and methoxy-substituted ligands were used, but introduction of electron-withdrawing substituents at the *para*-position resulted in decreased activity and diastereoselectivity, Table 31, entries 8 and 9. The most diastereoselective catalysts were obtained using ligands containing two *meta*-substituents on the phenyl rings, entries 6 and 7.

Schmid and colleagues tested derivatives of MeO-BIPHEP **76** in the enantioselective hydrogenation of several unconventional substrates [49]. Electronic effects on reaction rate and enantioselectivity were apparent in the asymmetric hydrogenation of the α-pyridyl ketone **77** to provide

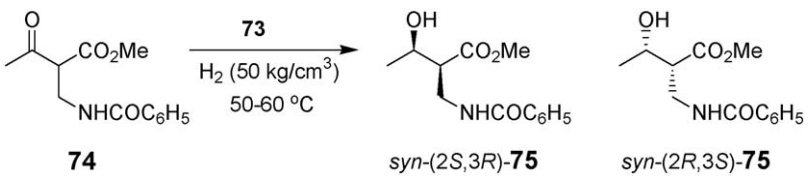

Scheme 38.

Table 31
Ru-catalysed hydrogenation of **24**

Entry	Catalyst	S/C	Solvent	Time (h)	Conv. (%)	De[a] (%)	Ee[b] (%)	Config.
1	**73a**	100	MeOH	40	100	51	97	2*R*,3*S*
2	**73b**	1000	MeOH	20	97	67	91	2*S*,3*R*
3	**73c**	1000	MeOH[c]	20	47	48	95	2*R*,3*S*
4	**73d**	1000	MeOH	20	94	67	91	2*R*,3*S*
5	**73e**	1000	MeOH	43	73	73	91	2*R*,3*S*
6	**73e**	1000	CH_2Cl_2–MeOH[d]	46	72	91	98	2*R*,3*S*
7	**73e**	100	CH_2Cl_2	40	68	95	99	2*R*,3*S*
8	**73g**	1000	MeOH[c]	20	20	39	94	2*R*,3*S*
9	**73h**	1000	MeOH	20	39	72	96	2*R*,3*S*
10	**73f**	1000	CH_2Cl_2–MeOH	40	55	98	99	2*S*,3*R*

[a] Determined by HPLC.
[b] Determined by HPLC analysis of (+)-MTPA ester of product.
[c] Water (0.5% v/v) added to MeOH.
[d] Ratio CH_2Cl_2:MeOH 7:1.

(*R*, *S*)-mefloquine **80**, the racemic version of which acts as an anti-malarial drug, Scheme 39.

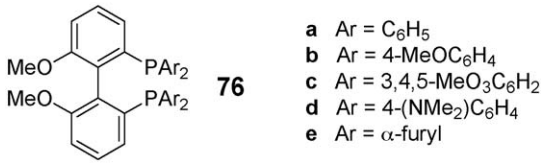

The parent MeO-BIPHEP afforded an ee of 71% but the conversion rate was slow, Table 32. Electron-donating phenyl-ring substituents in the *para*- or *ortho*-positions had a positive effect on enantioselectivity but more so on catalyst activity. The use of electron-withdrawing substituents led to complete loss of hydrogenation activity.

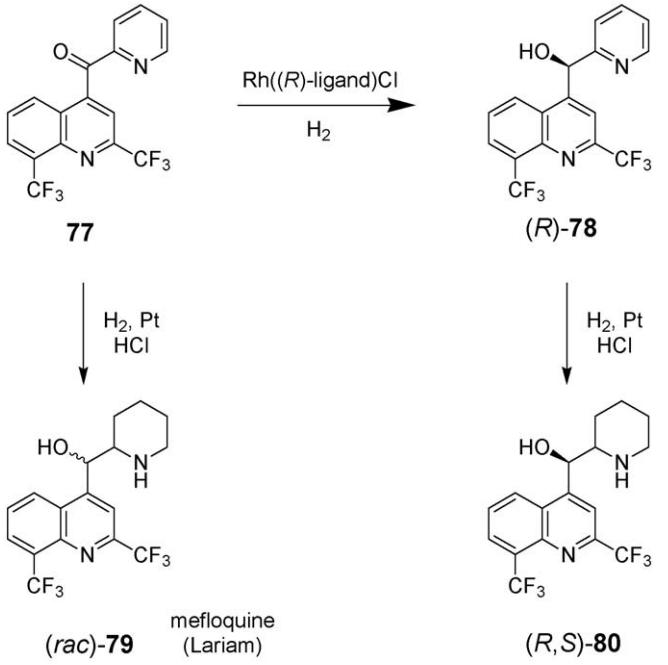

Scheme 39.

Table 32
Ru-catalysed hydrogenation of α-pyridyl ketone **77**

Entry[a]	Ligand	Conv.[b] (%)	Ee (%)
1	**76a**	10	71
2	**76b**	35	70
3	**76c**	44	85
4	**76d**	76	68

[a] S/C 200, toluene, $c = 1\%$, 60 °C, 60 bar.
[b] Conversion after 1 h.

Dihydrogeranylacetone **81** was also investigated as a substrate for the hydrogenation catalysed by Ru-complexes of the ligands derived from **76a–e**. High chemoselectivity in favour of reduction of the olefin, to yield **82**, rather than the ketone, which gives **83**, was required, Scheme 40. Hydrogenation promoted by Ru-BINAP and Ru-MeO-BIPHEP dimers was highly chemoselective, but the enantioselectivities were moderate, 64% and 77%, respectively. Inclusion of electron-releasing substituents on the MeO-BIPHEP phenyl rings led to improved rates but also to increased amounts of ketone reduction. High enantiomeric excesses were obtained using the 3,5-bis(*t*-Bu)-substituted and 3,5-bis(trimethylsilyl)-substituted ligands but the desired product was the minor one. Finally, it was the α-furyl-substituted MeO-BIPHEP analogue **76e** that afforded the best chemoselectivity and ee of 98% and 91%, respectively.

The precise reasons for enhanced results using the α-furyl substituted ligand were not elucidated, but an X-ray structure of the Ru diacetato complex of (*R*)-α-furyl-MeO-BIPHEP revealed only small differences in comparison to that of the unsubstituted ligand. It was also reported that use of the β-furyl and α-thienyl analogues were less effective and so it was concluded that subtle steric and electronic factors influenced the reaction outcome.

While many of the aforementioned ligand series have involved substitution of phosphine aryl groups to alter the ligand basicity, there have been examples of varying the electronic nature of the biaryl backbone of diphos-

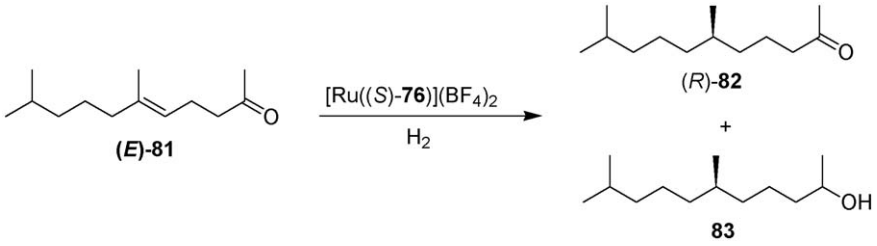

Scheme 40.

phines, Fig. 6. For comparison of performance of these ligands it is not only electronic effects that need to be taken into consideration, but also the effect on the structure of the metal complexes derived from the ligands. In particular, the steric demands due to ligand bite angle has a major role to play in catalyst activity and selectivity. It has been determined by several research groups that narrow bite angles (and therefore dihedral angles) are desirable for achieving high enantioselectivity in metal-catalysed hydrogenations [50–52]. As regards the electronic nature of the ligand, the majority of the most successful diphosphines for asymmetric hydrogenation have possessed biaryl backbones that are more electron-rich than the parent BINAP ligand [49–51,53]. Fewer examples of effective electron-deficient ligands have been reported [54,55].

Genêt et al. recently designed the electronically deficient diphosphine, Difluorphos **87** [56]. Molecular mechanics were used to estimate the dihedral angle of the ligand and to compare it to those of the four other diphosphines depicted in Fig. 6 including the closely related Segphos **86**. As had been expected, Segphos and Difluorphos displayed almost the same dihedral angle. This implied that a more valid comparison of the electronic effects of the two ligands could be made. The electronic profiles of the five ligands were established using NMR and IR techniques and Difluorphos was found to have the most π-acidic character, Fig. 7.

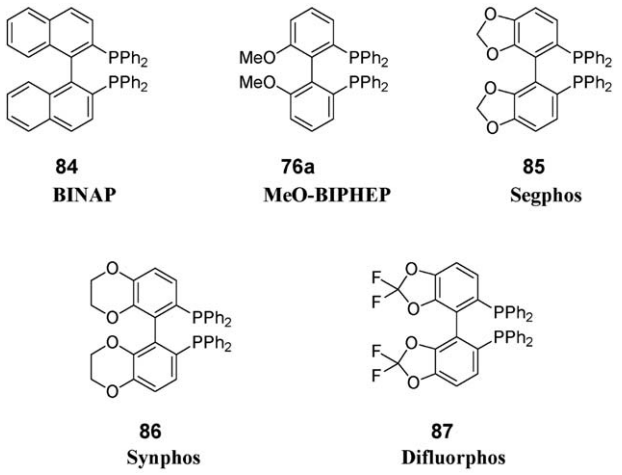

Fig. 6 Axially chiral diphosphine ligands.

Ruthenium-catalysts of enantiopure Difluorphos were applied in the asymmetric hydrogenation of β-keto esters, Table 33. After full conversion in all cases enantioselectivities were excellent and compared favourably to those obtained using other biaryl diphosphines. For instance, BINAP reduced ethyl benzoylacetate in only 88% ee compared to 92% ee generated with Difluorphos, entry 2. The reduction to ethyl (3*R*)-hydroxy-4-chlorobutyrate was also in good agreement with results previously achieved with BINAP- and Segphos-derived catalysts, entry 4 versus 5 and 6.

Attention then turned to more challenging electron-deficient substrates, which had in the past been reduced without much selectivity. The five diphosphines were all applied in the Ru-catalysed hydrogenation of the substrates **88a**–**c** under identical conditions, Scheme 41 and Table 34.

For **88a** and **88b**, the enantioselectivities increased as the dihedral angle decreased. However, on comparison of the enantiomeric excesses obtained using Segphos **85** and Difluorphos **87**, which display almost identical dihedral angles, there was a significant increase in enantioselectivity using the more electron-deficient fluorinated ligand (59% ee versus 70% ee for substrate **88a** and 76% versus 81% for **88b**). Difluorphos also proved superior to the other ligands assessed in the hydrogenation of **88c**, yielding the reduced product in 86% de and 98% ee. The results obtained for the Ru-catalysed hydrogenation of substrates **88a**–**c** were the highest reported using diaryl diphosphines and were ascribed to the unusual combination of narrow dihedral angle and high π-acidity.

Axially chiral phosphinamine ligands have also met with considerable success in asymmetric catalysis, in many cases exceeding the selectivity-inducing capabilities of their diphosphine analogues. This is exemplified by the application of the P,N ligand QUINAP **91** in the enantioselective hydroboration of a broader range of vinylarenes than was possible with BINAP. In a study by Brown, several QUINAP derivatives bearing different phosphorus aryl groups were synthesised and their rhodium complexes used for the asymmetric hydroboration of an extensive range of vinylarenes [58]. It was found that the parent QUINAP ligand induced the highest enantioselectivities for electron-rich substrates but for electronically deficient styrene derivatives the relatively electron-poor difurylphosphine ligand **92** was superior. It was stated that the assessment

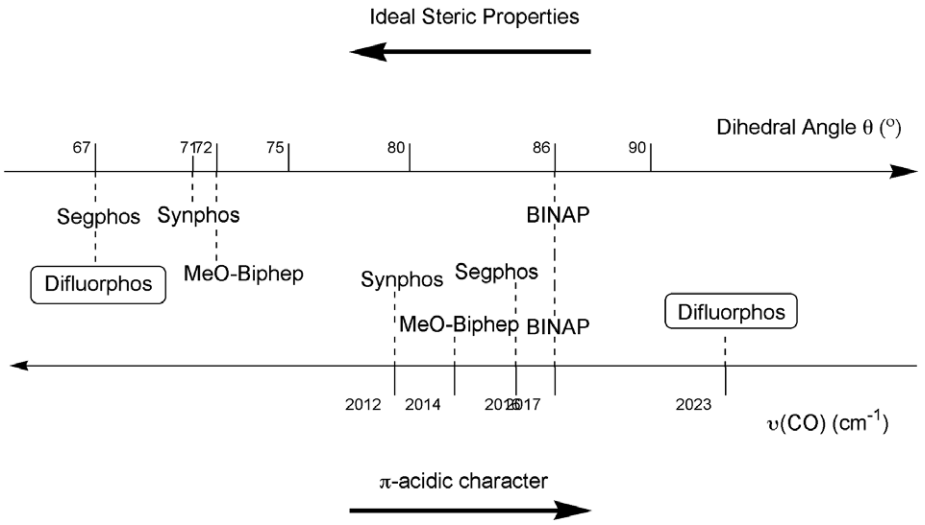

Fig. 7. Electronic profiles of selected axially chiral diphosphines.

of electronic effects can be hindered owing to the influence of both conjugative and inductive effects and that torsion-angles and molar volumes of chelated diphenylphosphines differ from those of difurylphosphines. However, Brown ventured to suggest that the results observed could be due to the difuryl-substituted ligand encouraging forma-

Table 33
Ru-catalysed hydrogenation of β-keto esters

Entry[a]	Substrate	Ligand	Solvent	pH_2 (bar)	Temperature (°C)	Time (h)	Ee[b] (%)
1	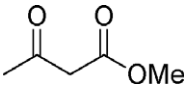	(*S*)-**87**	MeOH	4	50	24	99 (*S*)
2	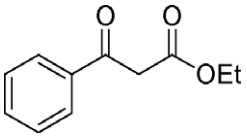	(*R*)-**87**	EtOH	10	80	24	92 (*S*)
3	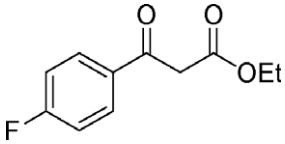	(*R*)-**87**	MeOH	10	80	24	95 (*S*)
4	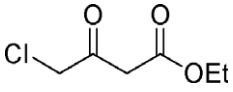	(*S*)-**84**	EtOH	10	110	3	97 (*S*)
5[c]	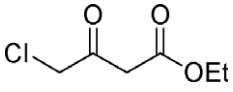	(*S*)-**86**		100	100		97 (*S*)
6[d]	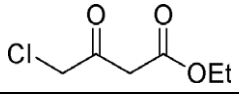	(*R*)-**86**		30	90		98 (*S*)

[a] Reactions carried out on a 1 mmol scale, 1 mol% [$RuBr_2$((*R*)or (*S*)-difluorphos)].
[b] Determined by chiral GC.
[c] Ref. [57].
[d] Ref. [50].

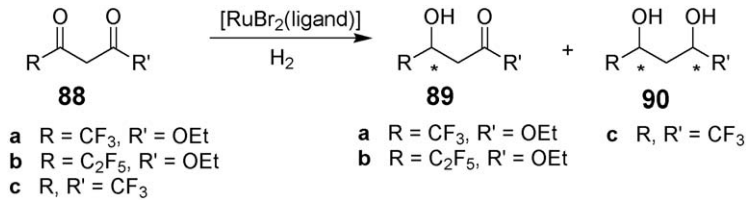

Scheme 41.

Table 34
Ru-catalysed hydrogenation of β-keto esters

Substrate	Conditions	Ee (%)					Product config.
		84	**76a**	**86**	**85**	**87**	
88a	10 bar, 110 °C, 1 h, EtOH	23	40	49	59	70	*R*
88b	10 bar, 110 °C, 1 h, EtOH	44	57	63	76	81	*R*
88c	50 bar, 50 °C, 24 h, MeOH	91 (de = 77%)	87 (de = 71%)	85 (de = 67%)	88 (de = 71%)	98 (de = 86%)	*R*, *R*

tion of a particular penta-coordinated rhodium complex wherein the electron-poor vinylarene substrate occupies a position that gives rise to enhanced enantioselective induction.

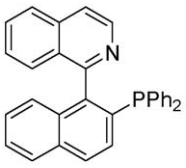

91

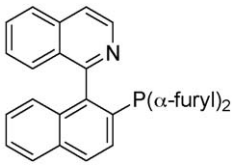

92

8. Conclusion

Variation of the electronic character of chiral ligands employed in asymmetric catalysis can have a profound effect on the course and outcome of the reaction. The extent to which the electronic influence is implemented as changes in the ratio and/or relative reactivity of diastereomeric intermediates or as alterations in mechanistic pathway is dependent on the reaction under investigation. However, the exact origin of these electronic effects remains difficult to study in isolation owing to possible masking by substrate and steric effects. Even after minimisation of these other contributing influences, a lack of detailed knowledge of the mechanisms of a number of catalytic processes and of the structures of the key intermediates involved therein, limits our understanding of the precise manner in which electronic perturbations of the ligand affect catalytic transformations. Despite these uncertainties, or perhaps in an effort to dispel them, substituent controlled electronic-tuning of ligands is becoming more widespread and, when used in tandem with positive steric influences, can be a powerful technique for achieving high selectivity in a range of valued metal-catalysed asymmetric reactions. It is clear that there will be many more reports of electronic effects in asymmetric catalysis in the future.

References

[1] E.N. Jacobsen, W. Zhang, M.L. Guler, J. Am. Chem. Soc. 113 (1991) 6703.
[2] M. Palucki, N.S. Finney, P.J. Pospisil, M.L. Guler, T. Ishida, E.N. Jacobsen, J. Am. Chem. Soc. 120 (1998) 948.
[3] K.M. Ryan, C. Bousquet, D.G. Gilheany, Tetrahedron Lett. 40 (1999) 3613.
[4] C.P. O'Mahony, E.M. McGarrigle, M.F. Renehan, K.M. Ryan, N.J. Kerrigan, C. Bousquet, D.G. Gilheany, Org. Lett. 3 (2001) 3435.
[5] A.M. Daly, M.F. Renehan, D.G. Gilheany, Org. Lett. 3 (2001) 663.
[6] C. Bonaccorsi, S. Bachmann, A. Mezzetti, Tetrahedron: Asymmetry 14 (2003) 845.
[7] R.M. Stoop, S. Bachmann, M. Valentini, A. Mezzetti, Organometallics 19 (2000) 4117.
[8] T.V. RajanBabu, A.L. Casalnuovo, J. Am. Chem. Soc. 114 (1992) 6265.
[9] T.V. RajanBabu, A.L. Casalnuovo, Pure Appl. Chem. 66 (1994) 1535.
[10] A.L. Casalnuovo, T.V. RajanBabu, T.A. Ayers, T.H. Warren, J. Am. Chem. Soc. 116 (1994) 9869.
[11] T.V. RajanBabu, T.A. Ayers, A.L. Casalnuovo, J. Am. Chem. Soc. 116 (1994) 4101.
[12] T.V. RajanBabu, B. Radetich, K.K. You, T.A. Ayers, A.L. Casalnuovo, J.C. Calabrese, J. Org. Chem. 64 (1999) 3429.
[13] T.V. RajanBabu, A.L. Casalnuovo, J. Am. Chem. Soc. 118 (1996) 6325.
[14] I. Gergely, C. Hegedus, H. Gulyas, A. Szollosy, A. Monsees, T. Riermeier, J. Bakos, Tetrahedron: Asymmetry 14 (2003) 1087.
[15] I. Gergely, C. Hegedus, A. Szollosy, A. Monsees, T. Riermeier, J. Bakos, Tetrahedron Lett. 44 (2003) 9025.
[16] C. Hegedus, J. Madarasz, I. Gergely, A. Szollosy, A. Monsees, T. Riermeier, J. Bakos, Tetrahedron: Asymmetry 15 (2004) 2507.
[17] S.-F. Zhu, Y. Fu, J.-H. Xie, B. Liu, L. Xing, Q.-L. Zhou, Tetrahedron: Asymmetry 14 (2003) 3219.
[18] Y. Fu, G.-H. Hou, J.-H. Xie, L. Xing, L.-X. Wang, Q.-L. Zhou, J. Org. Chem. 69 (2004) 8157.
[19] A. Korostylev, A. Monsees, C. Fischer, A. Borner, Tetrahedron: Asymmetry 15 (2004) 1001.

[20] M. van den Berg, A.J. Minnaard, E.P. Schudde, J. van Esch, A.H.M. de Vries, J.G. de Vries, B.L. Feringa, J. Am. Chem. Soc. 122 (2000) 11539.
[21] U. Nettekoven, M. Widhalm, P.C.J. Kamer, P.W.N.M. van Leeuwen, Tetrahedron: Asymmetry 8 (1997) 3185.
[22] U. Nettekoven, M. Widhalm, H. Kalchhauser, P.C.J. Kamer, P.W.N.M. van Leeuwen, M. Lutz, A.L. Spek, J. Org. Chem. 66 (2001) 759.
[23] U. Nettekoven, P.C.J. Kamer, M. Widhalm, P.W.N.M. van Leeuwen, Organometallics 19 (2000) 4596.
[24] H.L. Pedersen, M. Johannsen, J. Org. Chem. 67 (2002) 7982.
[25] X. Hu, H. Dai, X. Hu, H. Chen, J. Wang, C. Bai, Z. Zheng, Tetrahedron: Asymmetry 13 (2002) 1687.
[26] A. Schnyder, L. Hintermann, A. Togni, Angew. Chem., Int. Ed. Engl. 34 (1995) 931.
[27] A. Schnyder, A. Togni, U. Wiesli, Organometallics 16 (1997) 255.
[28] L.-X. Dai, T. Tu, S.-L. You, W.-P. Deng, X.-L. Hou, Acc. Chem. Res. 36 (2003) 659.
[29] T. Tu, W.-P. Deng, X.-L. Hou, L.-X. Dai, X.-C. Dong, Chem. Eur. J. 9 (2003) 3073.
[30] T. Tu, X.-L. Hou, L.-X. Dai, J. Organomet. Chem. 689 (2004) 3847.
[31] H. Nishiyama, S. Yamaguchi, M. Kondo, K. Itoh, J. Org. Chem. 57 (1992) 4306.
[32] S.-B. Park, K. Murata, H. Matsumoto, H. Nishiyama, Tetrahedron: Asymmetry 6 (1995) 2487.
[33] X.-W. Wu, K. Yuan, W. Sun, M.-J. Zhang, X.-L. Hou, Tetrahedron: Asymmetry 14 (2003) 107.
[34] J.P. Janssen, G. Helmchen, Tetrahedron Lett. 38 (1997) 8025.
[35] F. Menges, M. Neuburger, A. Pfaltz, Org. Lett. 4 (2002) 4713.
[36] C.A. Busacca, D. Grossbach, R.C. So, E.M. O'Brien, E.M. Spinelli, Org. Lett. 5 (2003) 595.
[37] Z. Herseczki, I. Gergely, C. Hegedus, A. Szollosy, J. Bakos, Tetrahedron: Asymmetry 15 (2004) 1673.
[38] C.P. Casey, E.L. Paulsen, E.W. Beuttenmueller, B.R. Proft, B.A. Matter, D.R. Powell, J. Am. Chem. Soc. 121 (1999) 63.
[39] C.P. Casey, E.L. Paulsen, E.W. Beuttenmueller, B.R. Proft, L.M. Petrovich, B.A. Matter, D.R. Powell, J. Am. Chem. Soc. 119 (1997) 11817.
[40] A. Saitoh, K. Achiwa, K. Tanaka, T. Morimoto, J. Org. Chem. 65 (2000) 4227.
[41] K. Inoguchi, S. Sakurba, K. Achiwa, Synlett (1992) 169.
[42] K. Kitayama, Y. Uozomi, T. Hayashi, J. Chem. Soc., Chem. Commun. (1995) 1533.
[43] T. Hayashi, S. Hirate, K. Kitayama, H. Tsuji, A. Torii, Y. Uozumi, Chem. Lett. (2000) 1272.
[44] T. Hayashi, S. Hirate, K. Kitayama, H. Tsuji, A. Torii, Y. Uozomi, J. Org. Chem. 66 (2001) 1441.
[45] P.J. Guiry, M. McCarthy, Tetrahedron 57 (2001) 3809.
[46] K. Mashima, K. Kusano, T. Ohta, R. Noyori, H. Takaya, J. Chem. Soc., Chem. Commun. (1989) 1208.
[47] K. Mashima, Y. Matsumura, K. Kusano, H. Kumobayashi, N. Sayo, Y. Hori, T. Ishizaki, S. Akutagawa, H. Takaya, J. Chem. Soc., Chem. Commun. (1991) 609.
[48] K. Mashima, K. Kusano, N. Sato, Y. Matsumura, K. Nozaki, H. Kumobayashi, N. Sayo, Y. Hori, T. Ishizaki, S. Akutagawa, H. Takaya, J. Org. Chem. 59 (1994) 3064.
[49] R. Schmid, E.A. Broger, M. Cerghetti, Y. Crameri, J. Foricher, M. Lalonde, R.K. Muller, M. Scalone, G. Schoettel, U. Zutter, Pure Appl. Chem. 68 (1996) 131.
[50] T. Saito, T. Yokozawa, T. Ishizaki, T. Moroi, N. Sayo, T. Miura, H. Kumobayashi, Adv. Syn. Catal. 343 (2001) 264.
[51] Z. Zhang, H. Qian, J. Longmire, X. Zhang, J. Org. Chem. 65 (2000) 6223.
[52] S. Duprat de Paule, S. Jeulin, V. Ratovelomanana-Vidal, J.-P. Genet, N. Champion, P. Dellis, Eur. J. Org. Chem. 68 (2003) 1931.
[53] C.C. Pai, Y.M. Li, Z.Y. Zhou, A.S.C. Chan, Tetrahedron Lett. 43 (2002) 2789.
[54] N.G. Andersen, M. Parvez, B.A. Keay, Org. Lett. 2 (2000) 2817.
[55] T. Benincori, E. Brenna, F. Sannicolo, L. Trimarco, E. Antognazza, E. Cesarotti, F. Demartin, T. Pilati, J. Org. Chem. 61 (1996) 6244.
[56] S. Jeulin, S. Duprat de Paule, V. Ratovelomanana-Vidal, J.-P. Genet, N. Champion, P. Dellis, Angew. Chem., Int. Ed. Engl. 43 (2004) 320.
[57] R. Noyori, Asymmetric Catalysis in Organic Synthesis, Wiley, New York, 1994, pp. 1–93.
[58] H. Doucet, E. Fernandez, T.P. Layzell, J.M. Brown, Chem. Eur. J. 5 (1999) 1320.